Simulation and Simplified Models for Turbulent Diffusion

Peter R. Kramer
Department of Mathematical Sciences
Rensselaer Polytechnic Institute

Two Uses of Simplified Models for Passive Scalar Transport

- Study Closure Approximations

- Analyze mean flow interaction with subgrid-scale turbulent fluctuations

Comparative Study of Closure Approximations

Joint work with Andy Majda, Eric Vanden-Eijnden.

Examine class of closure approximations founded on renormalized perturbation expansions

- Quasi-normal approximation (QNA) (various authors)
    - Linear, convolution in time
- Quasi-linear approximation (QLA) (van Kampen)
    - Linear, no convolution in time
- Direct Interaction Approximation (DIA) (Kraichnan)
    - Nonlinear, convolution in time
- Modified Direct Interaction Approximation (MDIA) (Vanden-Eijnden)
    - Nonlinear, no convolution in time
- Lagrangian Renormalized Approximation (LRA) (Corrsin, Kaneda)
    - Multiplicative nonlinearity, no convolution in time

Contents

- Mathematical Modeling Approach
- Results
- Mathematical Methods
- Conclusions

This complements numerical calculations on models, like Herring.

Mode of Investigation

Design a turbulent diffusion model which has:

- Sufficient simplicity to analyze in mathematically precise fashion
- Complex, nontrivial features
  - Difference between Eulerian and Lagrangian statistics
  - Flexibility to induce a variety of possible statistical behaviors for tracers
    - subdiffusion, ordinary diffusion, superdiffusion
    - Gaussian or persistently broader-than-Gaussian fluctuations in position (intermittency)

Calculate statistical quantities exactly and with closure methods and compare.

Previous Work

Methodology used by Avellaneda and Majda (1992) to examine QNA, DIA, and a renormalization group approach.

Present work uses model with more complex geometry

- shear flow with fluctuating cross sweep
- distinction between Eulerian and Lagrangian statisics
- previously utilized by K & Majda (1999) and Bourlioux & Majda (2001)

Focus on intermediate and long-time properties of tracer (passive scalar) transport.

Challenge of Model

Can the closure approximations even qualitatively replicate the correct statistics for single tracer motion?

Fundamental performance criteria:

- Mathematically meaningful (realizable) predictions
- Fundamental statistics computable
- Correct scaling of mean-square tracer displacement with time for subdiffusive, diffusive, and superdiffusive cases
- Correct prediction of whether the probability distribution function (PDF) for the tracer displacement is Gaussian, broader, or thinner
    - measured through flatness factor (ratio of fourth to second order moments)

Mathematical Realizability and Computability

DIA has following shortcomings in model:

- Unrealizable predictions when tracer motion subdiffusive
- Simple statistics, such as mean-square displacement along shear, given by equation more complicated than exact result and other closure approximations

Other methods exhibited no apparent inconsistencies or obstacles to computability in model.

Long-Time Rate of Growth of Mean-Square Tracer Displacement

Linear methods (QLA,QNA) sometimes qualitatively overpredict rate of tracer transport along shear

- Miss the inhibitory influence of the fluctuating cross sweep

Other methods correctly predict scaling of mean-square tracer displacement with respect to time.

- MDIA and LRA reproduce long-time asymptotics of mean-square tracer displacement exactly

Gaussian or Intermittent Tracer Displacement PDF

Only MDIA correctly predicts in all cases whether tracer displacement PDF has Gaussian, broader, or thinner shape.

- Moderate quantitative discrepancy

Random Shear Flow with Cross Sweep

(Avellaneda & Majda 1990, K & Majda 1999, Bourlioux & Majda 2001)

$$\vec{v}(x,y,t) = \begin{pmatrix} w(t) \\ v(x,t) \end{pmatrix}$$

- Gaussian statistics for $w(t)$ and $v(x,t)$
- Fairly arbitrary correlation structure
    - can include long-range or oscillatory correlations in space and time
- Lagrangian velocity statistics (observed by tracer) not equal to Eulerian velocity statistics (observed at fixed point)

Mathematical Equations for Advection-Diffusion

Advection-diffusion equation for passive scalar (concentration) density $T(\vec{x}, t)$

$$\frac{\partial T}{\partial t} + \vec{v}(\vec{x}, t) \cdot \nabla T = \kappa \Delta T,$$
$$T(\vec{x}, t = 0) = T_0(\vec{x}).$$

Velocity field $\vec{v}(\vec{x}, t)$, molecular diffusion $\kappa > 0$.

Equation of motion for tracers:

$$\begin{aligned} dX(t) &= w(t)\,dt + \sqrt{2\kappa}\,dW_x(t), \\ dY(t) &= v(X(t), t)\,dt + \sqrt{2\kappa}\,dW_y(t). \end{aligned}$$

with Brownian motion processes $W_x(t)$ and $W_y(t)$.

Explicit Solution of Tracer Trajectories

May assume $(X(0), Y(0)) = (0, 0)$:

$$X(t) = \int_0^t w(s)\,ds + \sqrt{2\kappa}\,W_x(t),$$
$$Y(t) = \int_0^t v(X(s), s)\,ds + \sqrt{2\kappa}\,W_y(t).$$

Can calculate many statistical quantities through averaging of functions of these expressions.

Sweeping motion along x direction causes streamline blocking and decorrelation of Lagrangian velocity along shear.

Flatness Factor along Sweeping Direction

$$F^*_{X,4} = \lim_{t\to\infty} \frac{\langle X^4(t)\rangle}{\left(\langle X^2(t)\rangle\right)}$$

is simplest measure of shape of tracer displacement PDF along x direction.

- Large values of $F^*_{X,4}$ associated to significant probability of large fluctuations.

  $F^*_{X,4} = 3$ for Gaussian statistics for tracer displacement.

  $F^*_{X,4} \geq 1$ for mathematical realizability.

Flatness Factor along Shearing Direction

$$F^*_{Y,4} = \lim_{t\to\infty} \frac{\langle Y^4(t)\rangle}{\left(\langle Y^2(t)\rangle\right)}$$

Consider special case:

- $\kappa > 0$,
- steady shear $v(x,t) = v(x)$,
- no cross sweep $w(t) = 0$.

Relative Complexity of Closure Approximations

- DIA equations most difficult to solve

- MDIA equations have complicated nonlinearity, but no convolution in time.
  - Less difficult to solve than DIA in present model.

- LRA equations have mild nonlinearity which is exactly solvable in model.

- QNA obeys linear equation with time convolution – solve by Laplace transform.

- QLA obeys linear, convolution-free equation; easily solved in model.

Conclusions

- Illustration of use of mathematical model to assess strengths and weaknesses of approximate methods

- MDIA had best fidelity in model

- RLA is a simpler method which performed adequately in model except for capturing intermittency

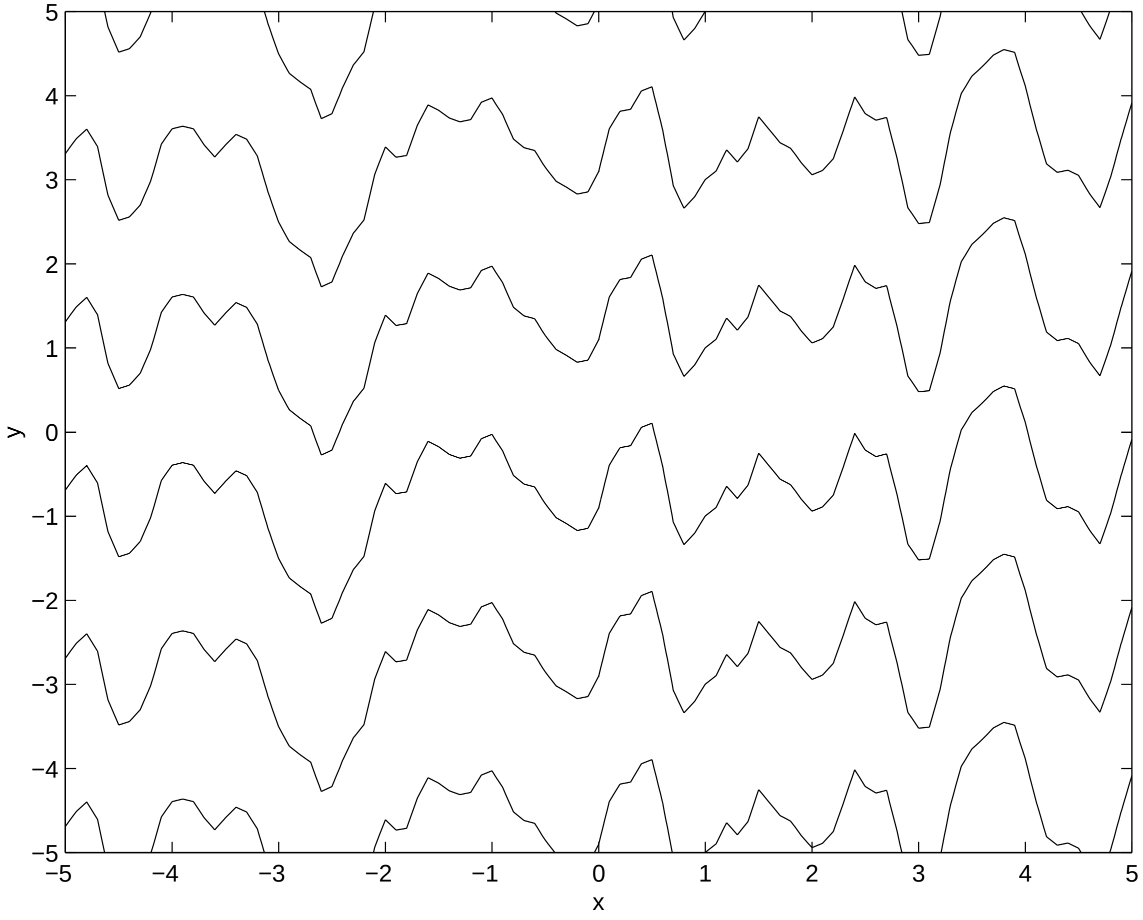

Figure 1: Streamlines of a shear flow with cross sweep.

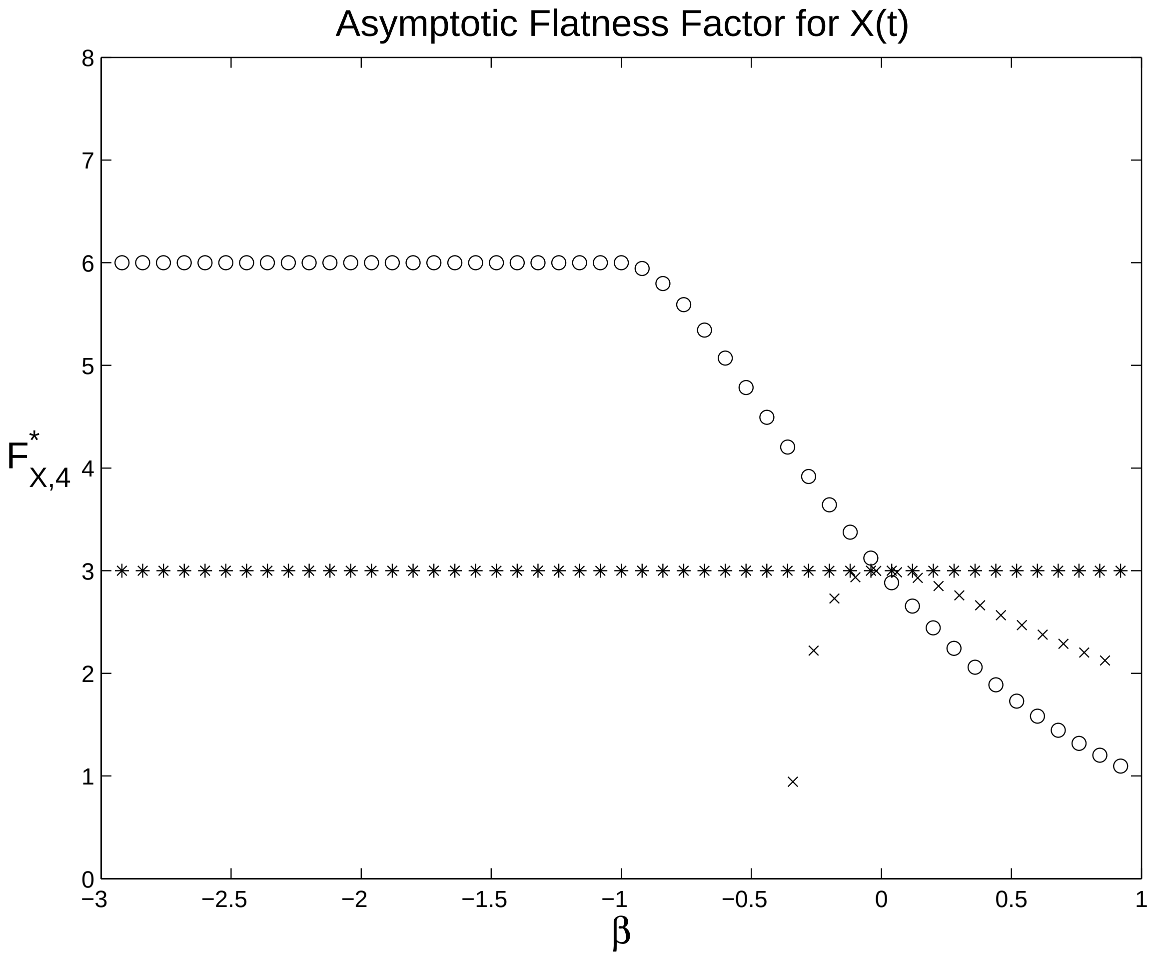

Figure 2: Asymptotic flatness factors along sweep, $F^*_{X,4}$. Exact, QLA, MDIA, LRA: stars '*', QNA: circles 'o', DIA: crosses 'x'.

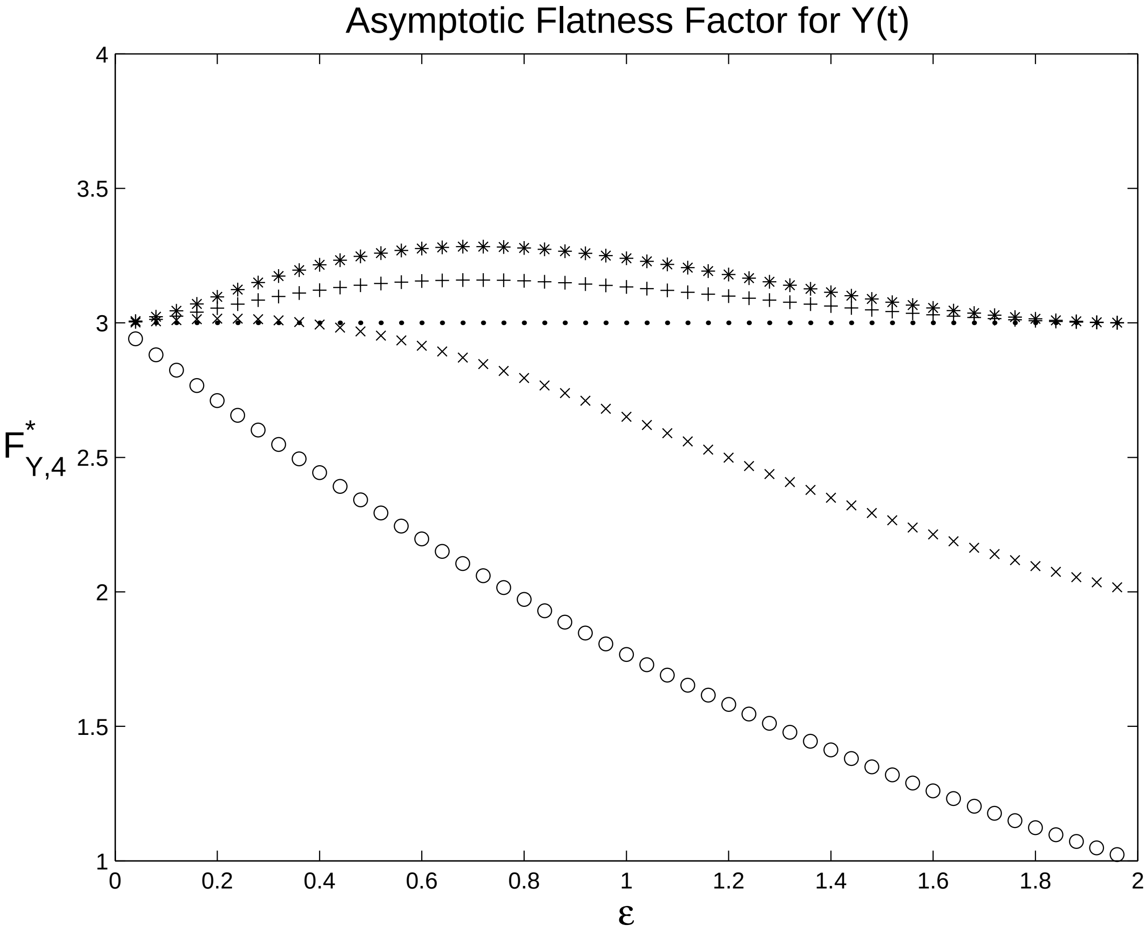

Figure 3: Asymptotic flatness factors $F^*_{Y,4}$ along shear. Exact: stars '*', QNA: circles 'o', QLA and LRA: dots '.', DIA: crosses 'x', MDIA: pluses '+'

Homogenized Transport by a Spatiotemporal Mean Flow with Small-Scale Periodic Fluctuations

Peter R. Kramer and Grigorios A. Pavliotis
Department of Mathematical Sciences
Rensselaer Polytechnic Institute

Contents

- Introduction
- Effective Large-Scale Equations
- Examples
- Conclusions

Goals of Investigation

- Simplified model to understand quantitatively the nonlinear coupling between mean flow and fluctuating velocity in determining tracer transport

- Build off previous work of Majda, McLaughlin, Bonn to include spatio-temporal dependence in mean flow

Qualitative Properties of Model

- Rigorous derivation of effective large-scale equations with "subgrid-scale" periodic fluctuations averaged out

- Effective diffusivity in large-scale equation depends in nonlinear way on mean flow, subgrid-scale fluctuations, and molecular diffusion

- Effective diffusivity varies in space and time when mean flow does
  - Variation can be rather dramatic

- A drift correction emerges from variability of effective diffusivity
  - Both symmetric and antisymmetric components contribute

Advection-Diffusion Equation

$$\frac{\partial T(\mathbf{x},t)}{\partial t} + \vec{u}(\vec{x},t)\cdot\nabla T(\mathbf{x},t) = \kappa\Delta T(\mathbf{x},t),$$
$$T(\mathbf{x},t=0) = T_0(\mathbf{x})$$

- Passive scalar field $T(\mathbf{x},t)$
- Velocity field $\vec{u}$ = large-scale mean flow + small-scale periodic fluctuations
- Molecular diffusion coefficient κ
- Some issues studied by Mazzino and collaborators (1997)

Nondimensionalization on Large Scales

$$\mathrm{St}_g \frac{\partial T(\mathbf{x},t)}{\partial t} + \left(\vec{V}(\vec{x},t) + a\vec{v}\left(\frac{\vec{x}}{\delta},\frac{t}{\eta}\right)\right) \cdot \nabla T(\mathbf{x},t)$$

$$= \mathrm{Pe}_g{}^{-1} \Delta T(\mathbf{x},t),$$

$$T(\mathbf{x},t=0) = T_0(\mathbf{x})$$

- Large-scale Strouhal number: St_g
- Large-scale Péclet number: Pe_g
- Ratios of small:large space,time, velocity scales: $\delta, \eta \ll 1$, $a \lesssim 1$

Large-Scale Effective Equation

- Different effective large-scale equations can emerge, depending upon the relationship between nondimensional parameters
- Interesting case where mean flow and fluctuations have comparable amplitude: $\eta = \delta$, $a = 1$, $\mathrm{Pe}_g = \delta^{-1}\,\mathrm{Pe}_\ell$, with $\mathrm{Pe}_\ell, \mathrm{St}_g \sim O(1)$.

Then for small but finite δ, obtain homogenized equation for approximate solution $\overline{T}$:

$$\mathrm{St}_g \frac{\partial \overline{T}(\mathbf{x},t)}{\partial t} + \mathbf{V}(\mathbf{x},t)\cdot\nabla\overline{T}(\mathbf{x},t) \\ = \delta\,\nabla\cdot(\mathcal{K}^*(\mathbf{x},t)\nabla\overline{T}(\mathbf{x},t)),$$

The effective diffusivity matrix is computed through cell problem on small-scale period:

$$\mathrm{St}_g \frac{\partial \chi_i}{\partial \tau} + (\mathbf{V}(\mathbf{x},t) + \mathbf{v}(\mathbf{y},t))\cdot\nabla_y\chi_i - \frac{1}{Pe_l}\Delta_y\chi_i \\ = -v_i(\mathbf{y},\tau), \quad i = 1,..,d$$

via

$$\mathcal{K}^*_{ij}(\mathbf{x},t) = \frac{1}{Pe_l}\,\delta_{ij} - \langle v_i\,\chi_j\rangle$$

Remarks on Homogenized Equation

- Previous work with constant or zero mean flow generated similar equation with constant effective diffusivity $\mathcal{K}^*$

- $\mathcal{K}^*$ inherits space-time dependence from that of $\vec{V}$

- Space-dependence of $\mathcal{K}^*$ generates drift correction $\nabla \cdot \mathcal{K}^*$.
  - Both symmetric and antisymmetric parts of $\mathcal{K}^*$ contribute to drift.

- Overall transport determined by nonlinear interaction of mean flow and effective diffusivity.

Derivation based on rigorous multiple-scale asymptotic expansion,

- Other distinguished limits give rise to variations of homogenized equations.

Variability of Effective Diffusivity

$\mathcal{K}^*$ depends on mean flow in delicate way (Koch et al 1989, Majda and McLaughlin 1993, Fannjiang and Papanicoloau 1994), particularly at large Pe_ℓ:

- direction of mean flow (production of resonant channels)
- locations where mean flow vanishes (local suppression or enhancement of effective diffusivity)

Examples

Steady, spatially linear large-scale mean flow:

$$\vec{V}(\vec{x}) = \begin{bmatrix} -\gamma\frac{1}{2} & \omega_0 \\ -\frac{1}{2}\omega_0 & \gamma \end{bmatrix} \begin{bmatrix} x_1 \\ x_2 \end{bmatrix};$$

represents generic local structure of incompressible flow

Steady cellular small-scale fluctuations:

$$\vec{v}(\vec{y}) = \begin{bmatrix} \partial\psi/\partial y_2 \\ -\partial\psi/\partial y_1 \end{bmatrix},$$

with $\psi = \sin 2\pi y_1 \sin 2\pi y_2$.

Solve cell problem numerically with spectral method, using the Biconjugate Gradient Stabilized method with incomplete LU factorization for preconditioning.

Childress-Soward Flow

Family of periodic fluctuations with both closed islands and open streaming regions:

$$\vec{v}(\vec{y}) = \begin{bmatrix} \partial\psi/\partial y_2 \\ -\partial\psi/\partial y_1 \end{bmatrix},$$

with $\psi = \sin 2\pi y_1 \sin 2\pi y_2 + \varepsilon \cos 2\pi y_1 \cos 2\pi y_2$.

Chaotic Flow (Biferale et al)

$$\vec{v}(\vec{y}) = \begin{bmatrix} \cos y_2 + \sin y_2 \cos t \\ \cos y_1 + \sin y_1 \cos t \end{bmatrix},$$

Childress-Soward Flow with Temporal Fluctuation

(Bonn and McLaughlin)

$$\vec{v}(\vec{y}) = \vec{w}(t) + \begin{bmatrix} \partial\psi/\partial y_2 \\ -\partial\psi/\partial y_1 \end{bmatrix},$$

with

- $\psi = \sin 2\pi y_1 \sin 2\pi y_2 + \varepsilon \cos 2\pi y_1 \cos 2\pi y_2$

- $$\vec{w}(t) = \begin{bmatrix} w_1 \sin(2\pi t) \\ w_2 \sin(2\pi t + \phi) \end{bmatrix}$$

Effective diffusivity not symmetric when $\phi \neq 0$.

Modified Cellular Flow

$$\vec{v}(\vec{y}) = \begin{bmatrix} \partial\psi/\partial y_2 \\ -\partial\psi/\partial y_1 \end{bmatrix},$$

with

$$\psi = \sin 2\pi y_1 \sin 2\pi y_2 + (\cos 2\pi y_1)^2$$

Effective diffusivity not symmetric.

Conclusions-Further Work

Mean flow and small-scale turbulent fluctuations interact on several levels in determining effective passive scalar transport.

Ongoing and future developments:

- Analytical characterization of “skew-flux”
- Homogenized equation for strong mean flows and other distinguished limits
- How does the interaction between the mean flow and the effective diffusivity affect the mixing and spreading properties of the passive scalar?
- Random homogenous small-scale fluctuations

Note that the mean shear flow is not always taken in the same direction.

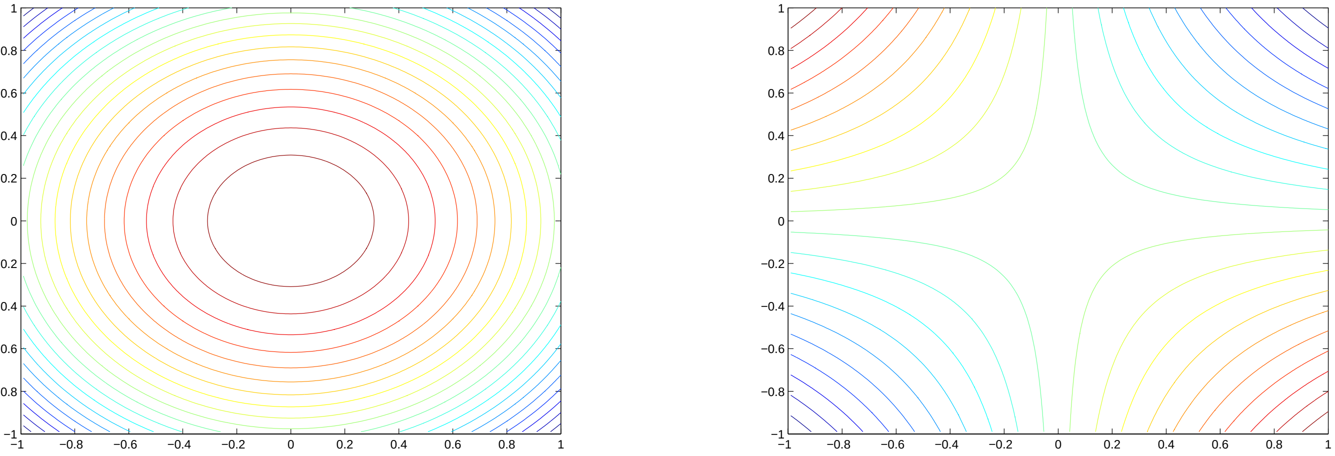

a. $\gamma = 0.0$, $\omega_0 = 10.0$ b. $\gamma = 10.0$, $\omega_0 = 0.0$

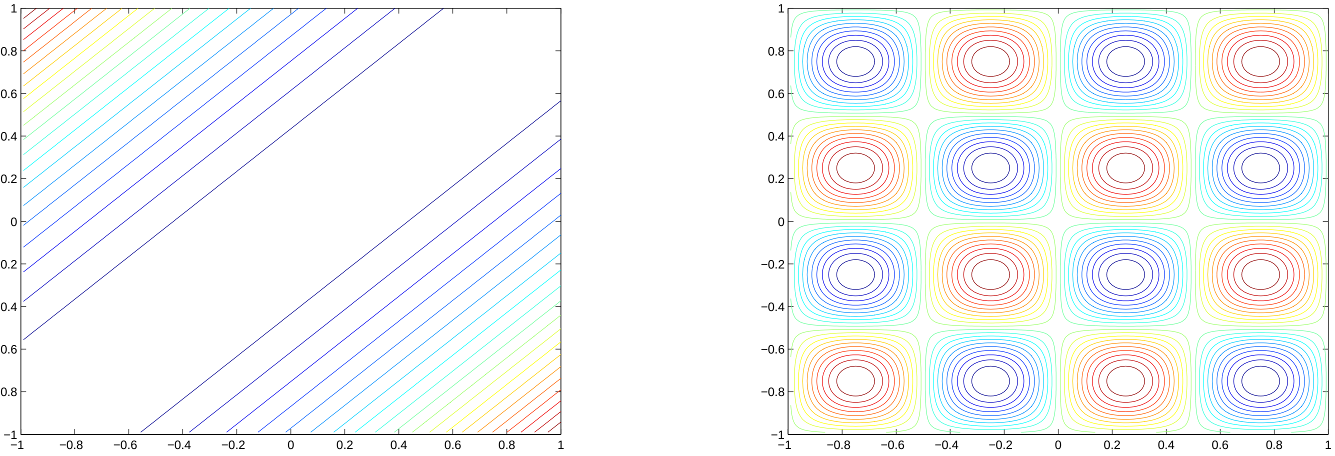

c. $\gamma = 5.0$, $\omega_0 = -10.0$ Cellular flow

Figure 1: Contour plots of the streamlines of mean flow and periodic fluctuations.

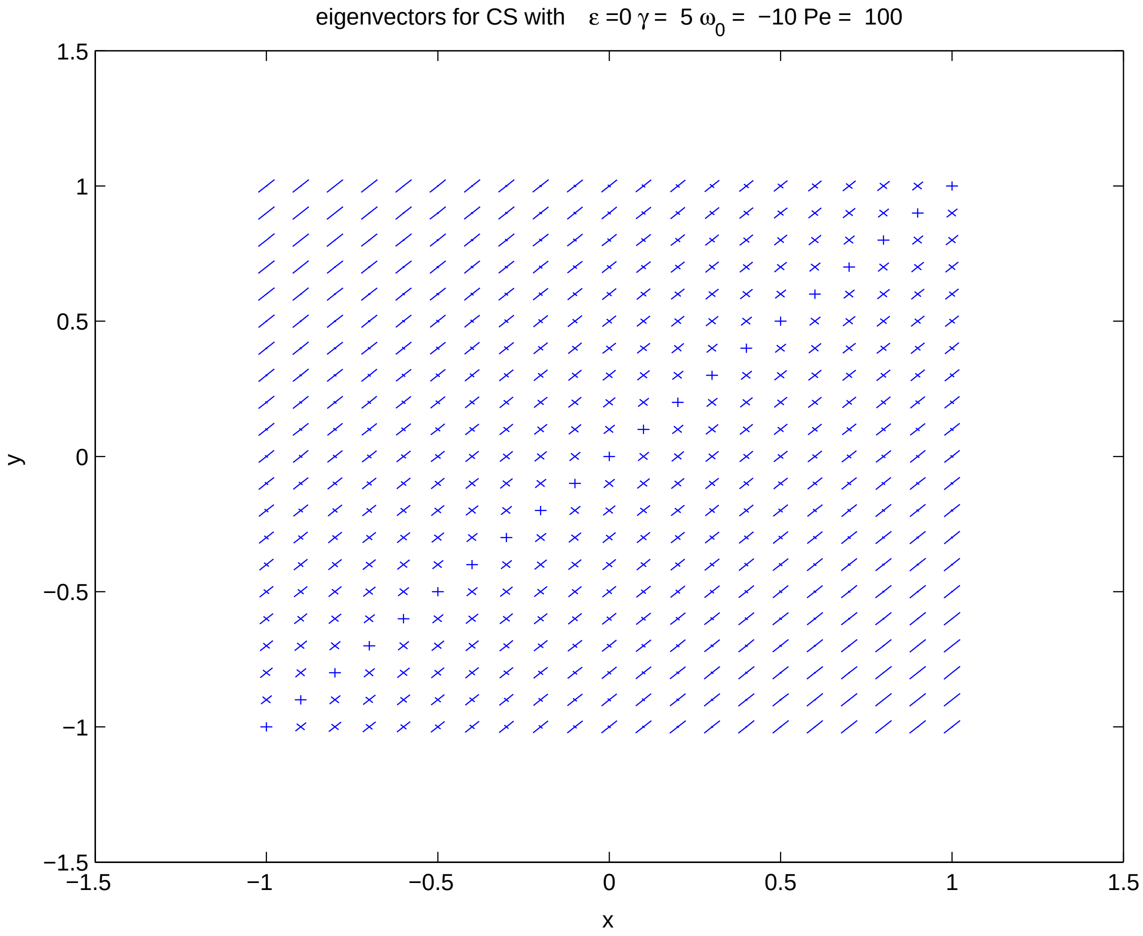

Figure 2: Effective diffusivity $\mathcal{K}^*$ in mean shear flow with cellular periodic fluctuations.

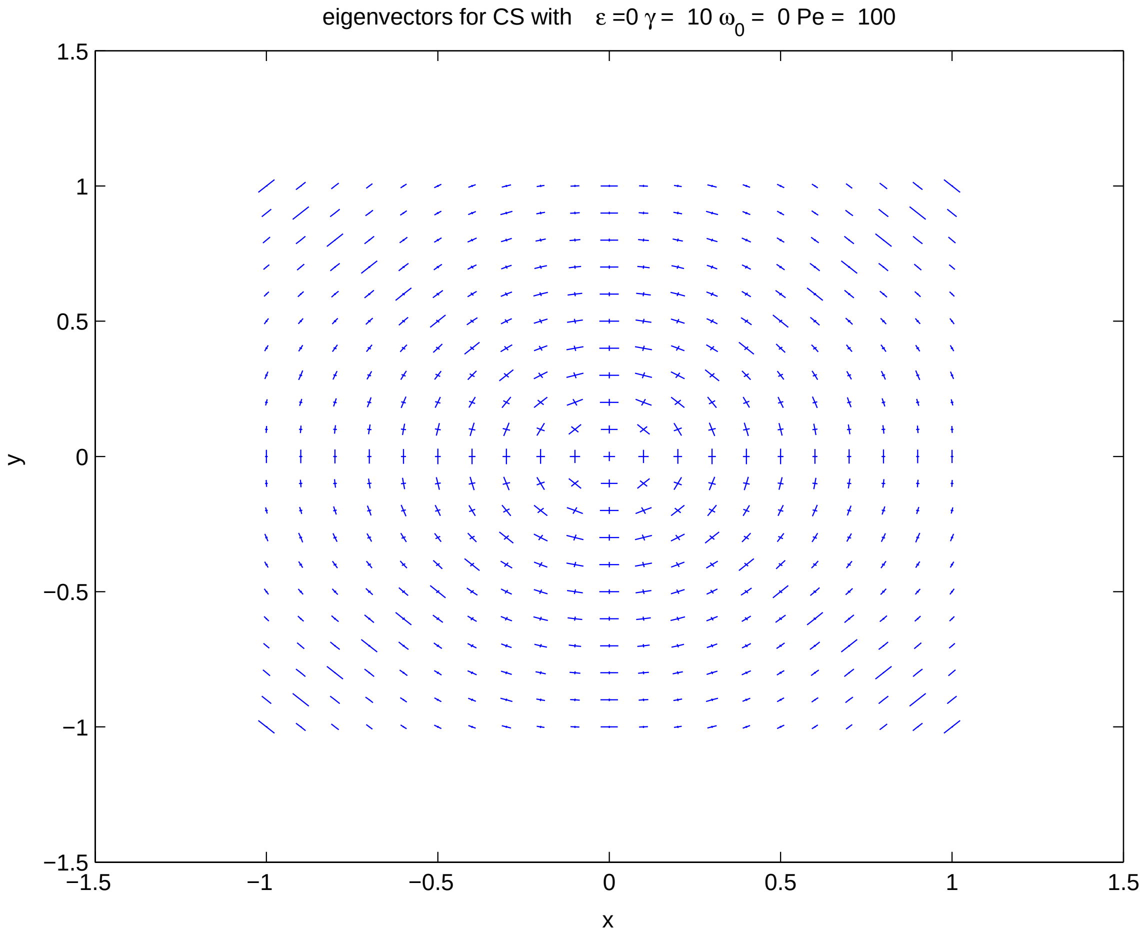

Figure 3: Effective diffusivity $\mathcal{K}^*$ in mean strain flow with cellular periodic fluctuations.

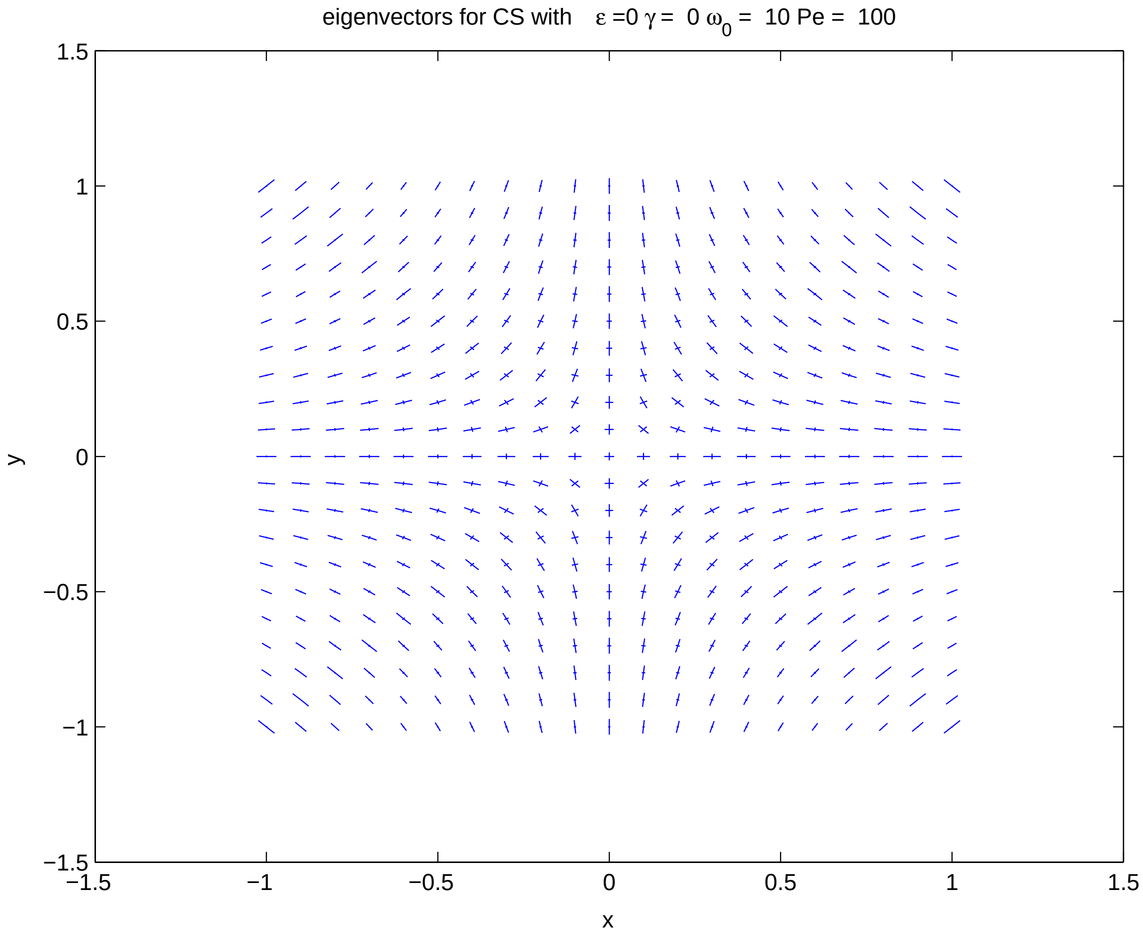

Figure 4: Effective diffusivity $\mathcal{K}^*$ in mean vortex flow with cellular periodic fluctuations.

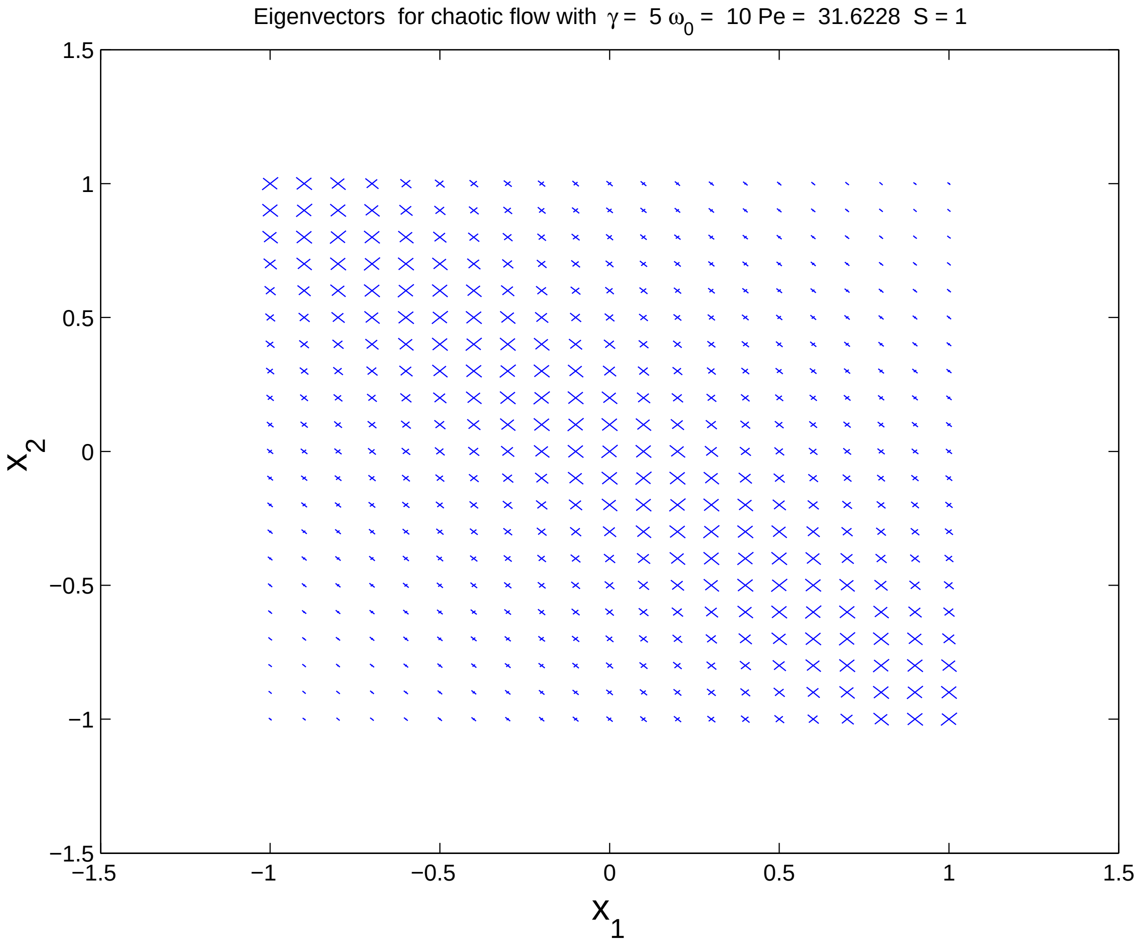

Figure 5: Effective diffusivity $\mathcal{K}^*$ in mean shear flow and chaotic periodic fluctuations.

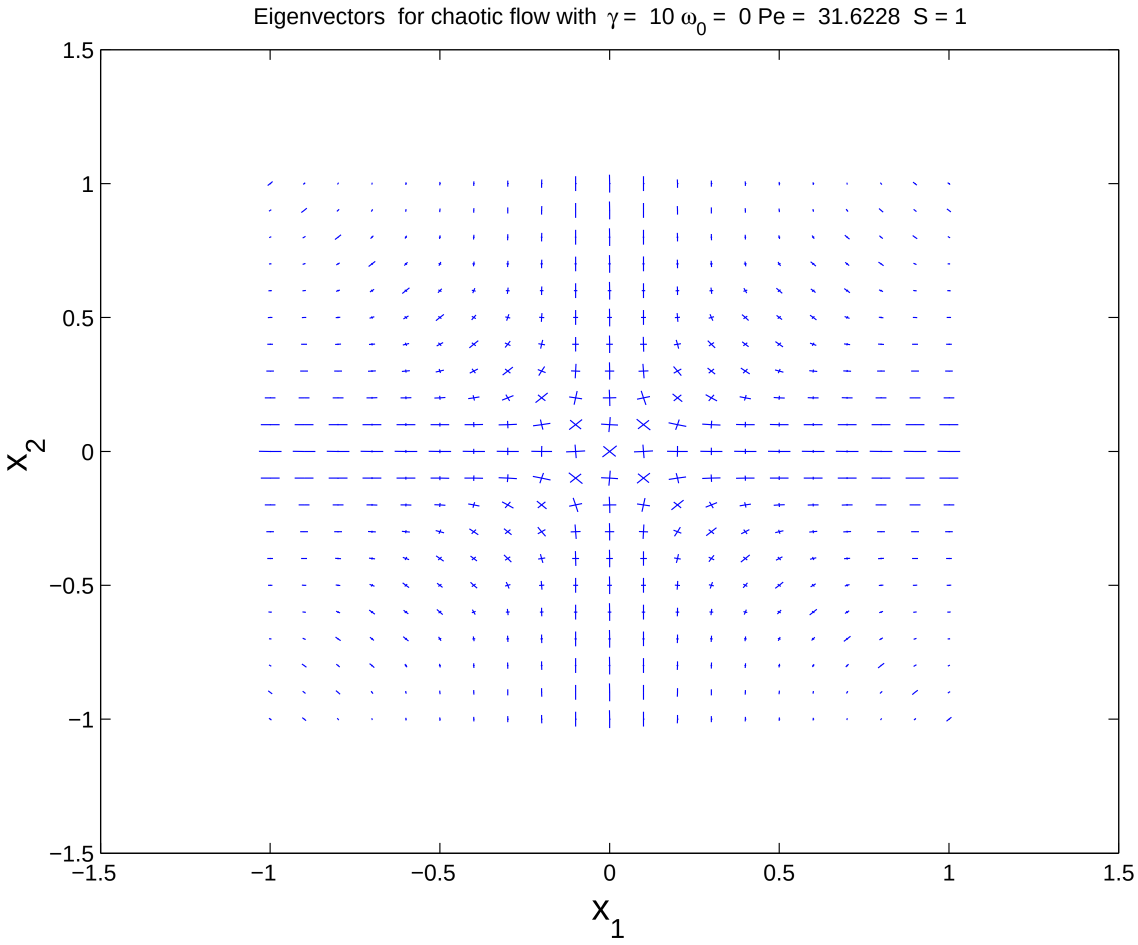

Figure 6: Effective diffusivity $\mathcal{K}^*$ in mean strain flow and chaotic periodic fluctuations.

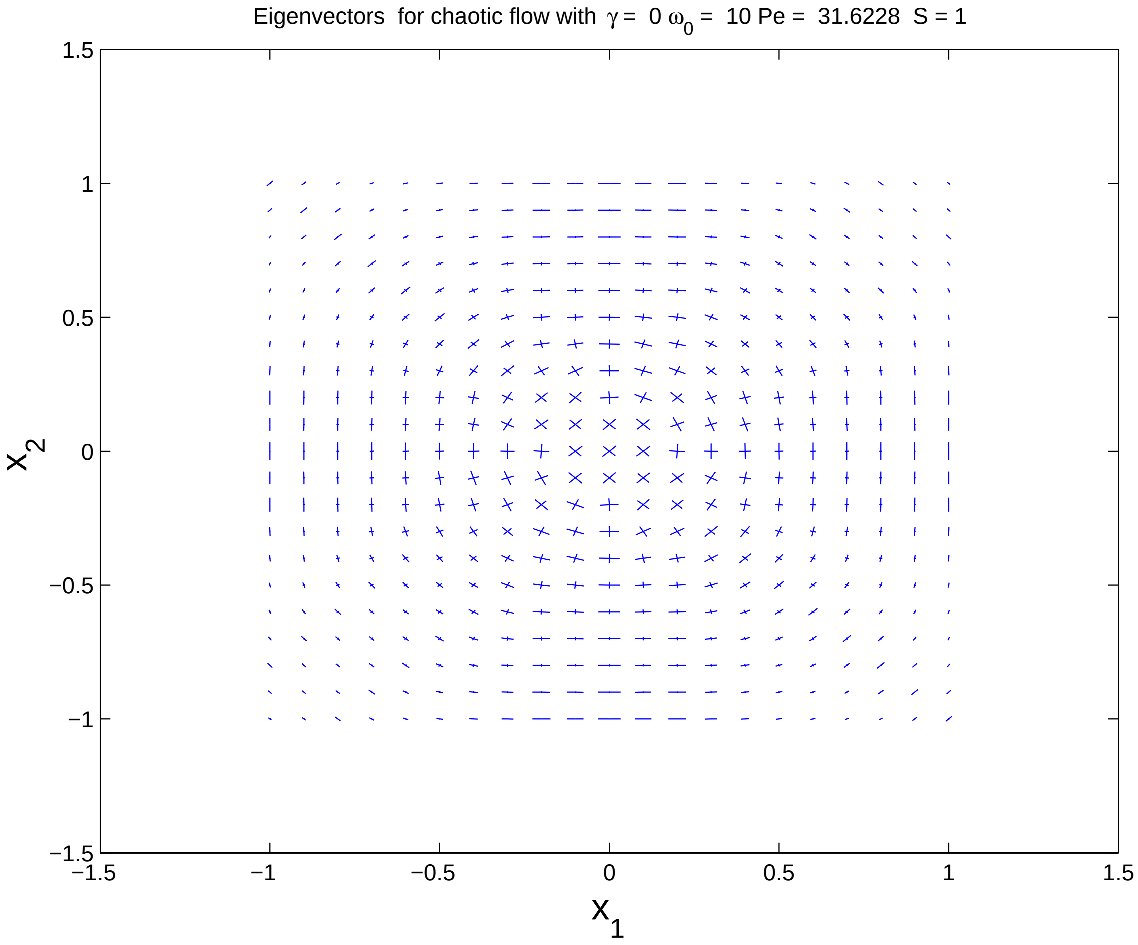

Figure 7: Effective diffusivity $\mathcal{K}^*$ in vortex flow with chaotic periodic fluctuations.

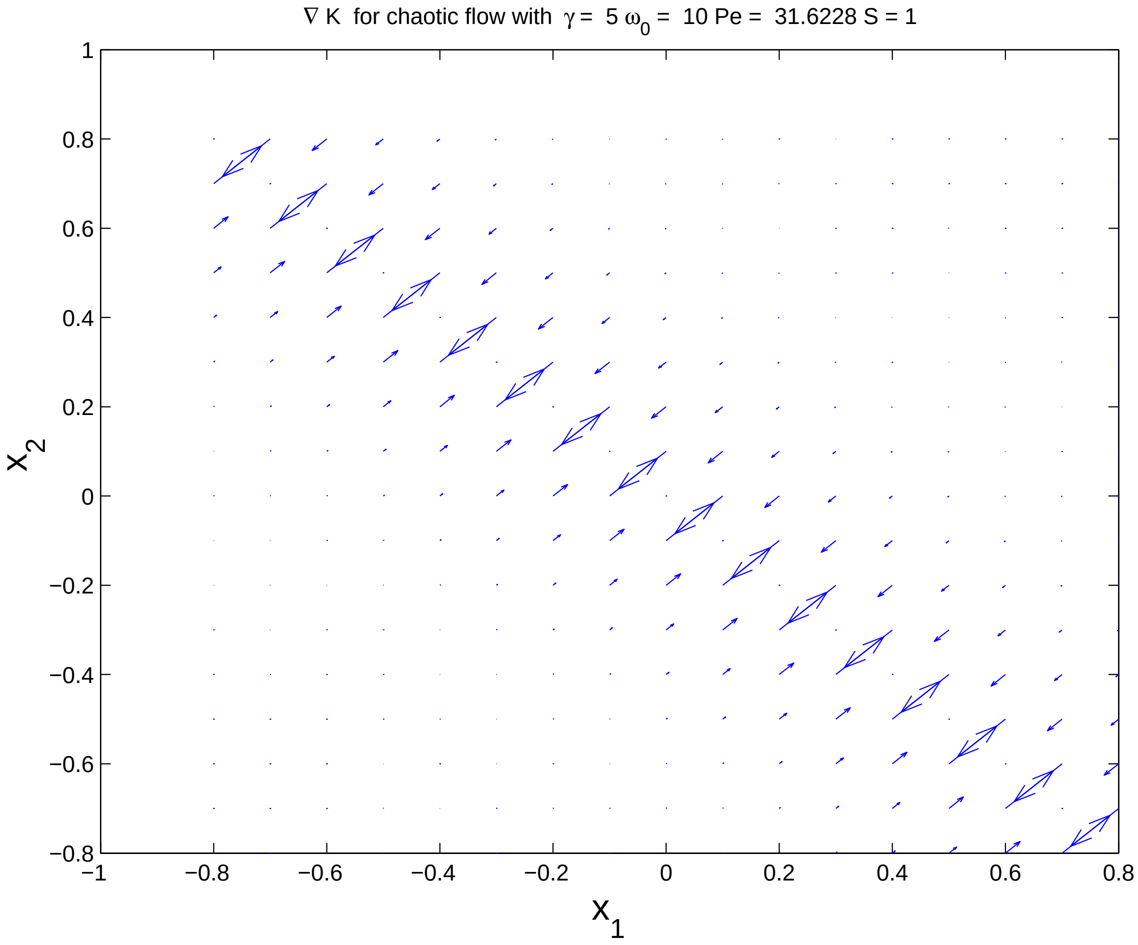

Figure 8: Drift correction $\nabla \cdot \mathcal{K}^*$ in mean shear flow and chaotic periodic fluctuations.

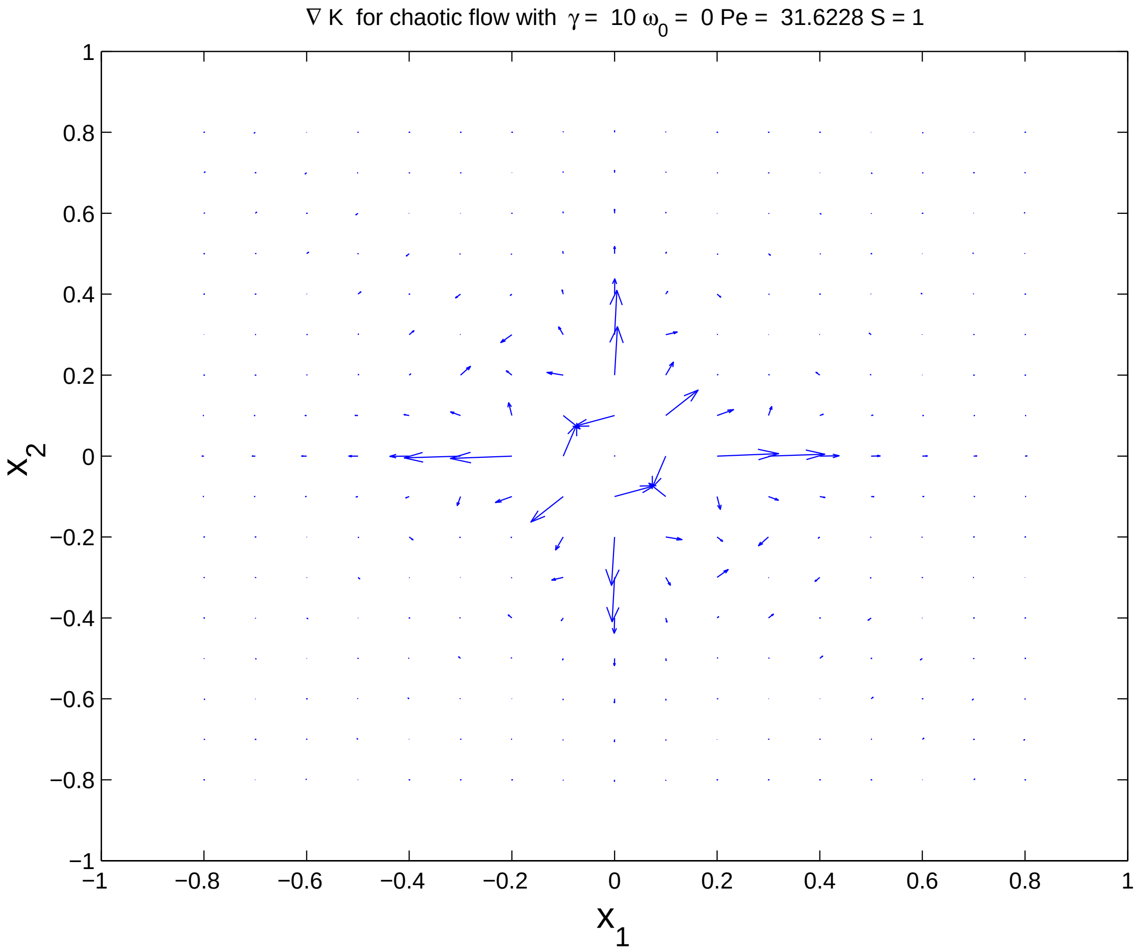

Figure 9: Drift correction $\nabla \cdot \mathcal{K}^*$ in mean strain flow and chaotic periodic fluctuations.

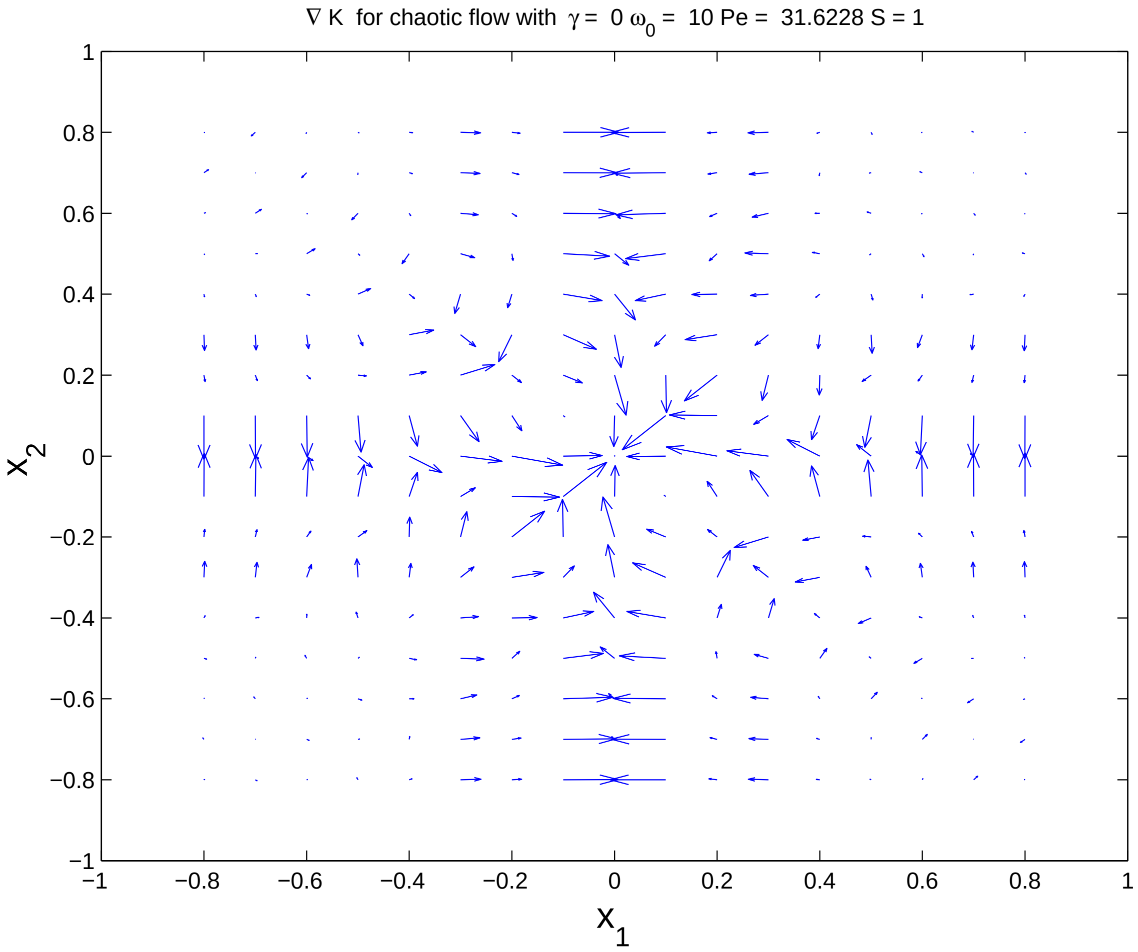

Figure 10: Drift correction $\nabla \cdot \mathcal{K}^*$ in mean vortex flow and chaotic periodic fluctuations.

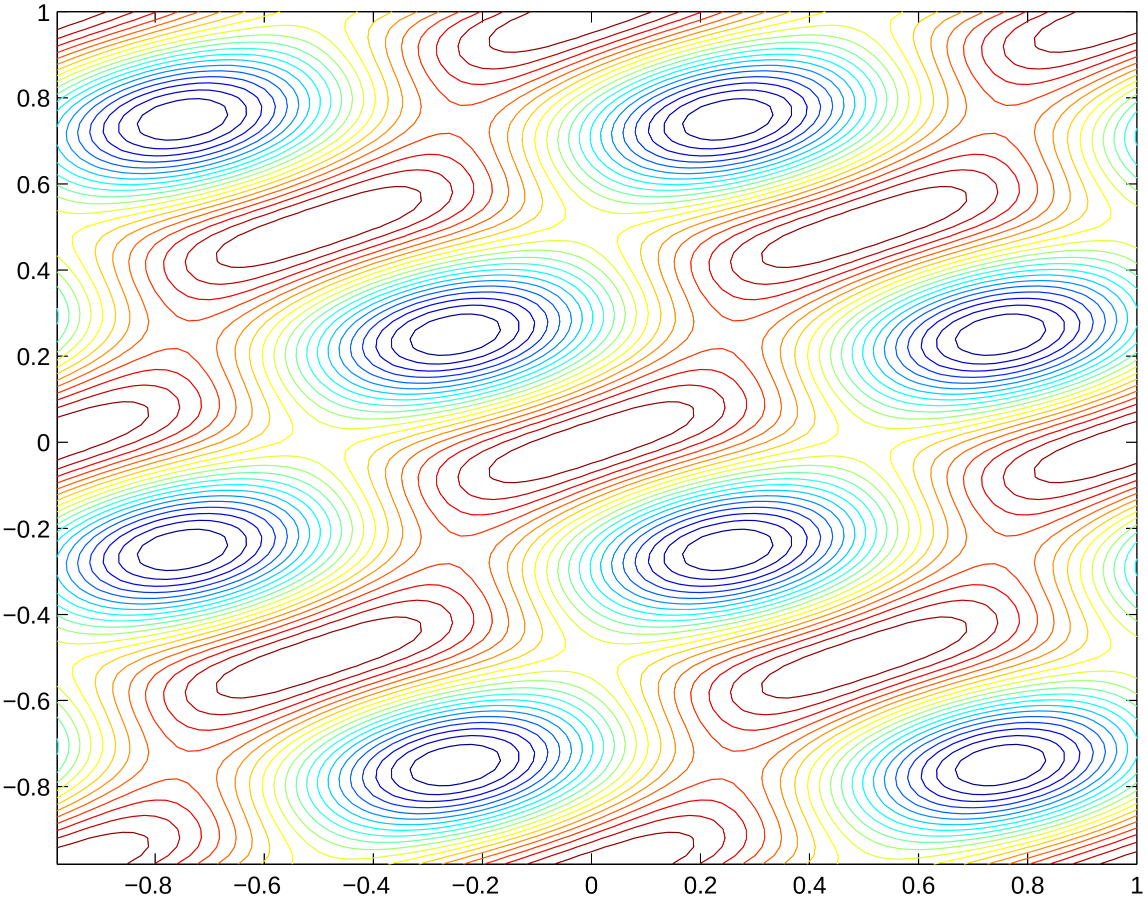

Figure 11: Streamlines of Modified Cellular flow $\psi = \sin 2\pi x_1 2\pi x_2 + (cos 2\pi x_1)^2$.

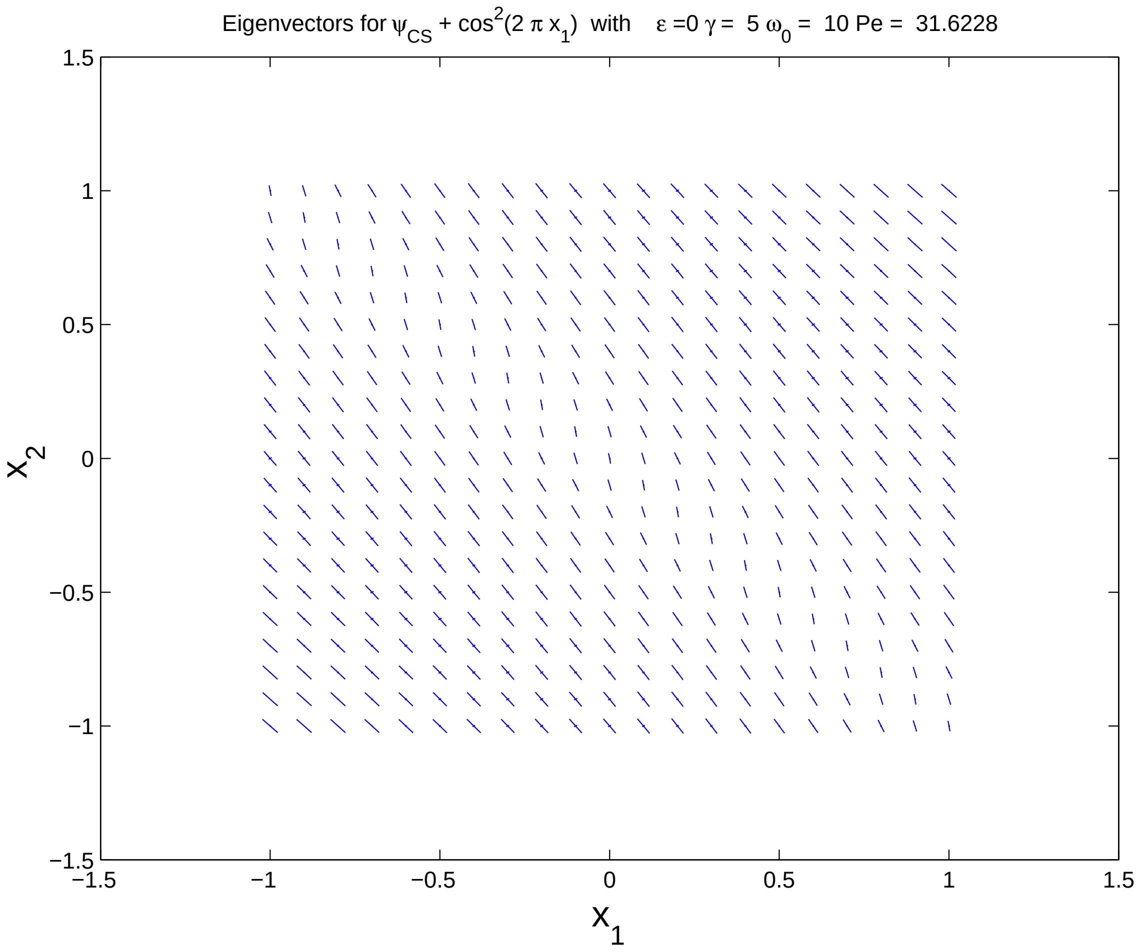

Figure 12: Effective diffusivity $\mathcal{K}^*$ in mean shear flow and modified cellular periodic fluctuations.

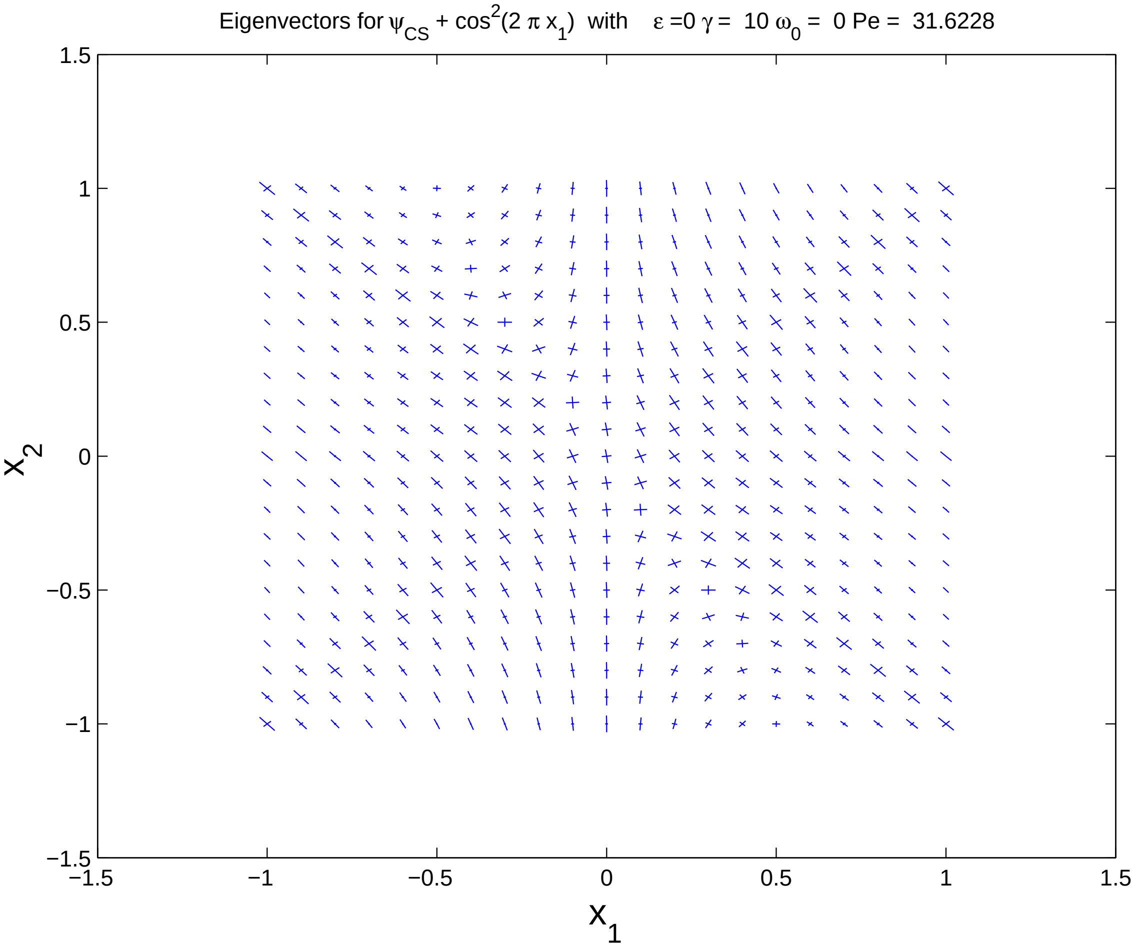

Figure 13: Effective diffusivity $\mathcal{K}^*$ in mean strain flow and modified cellular periodic fluctuations.

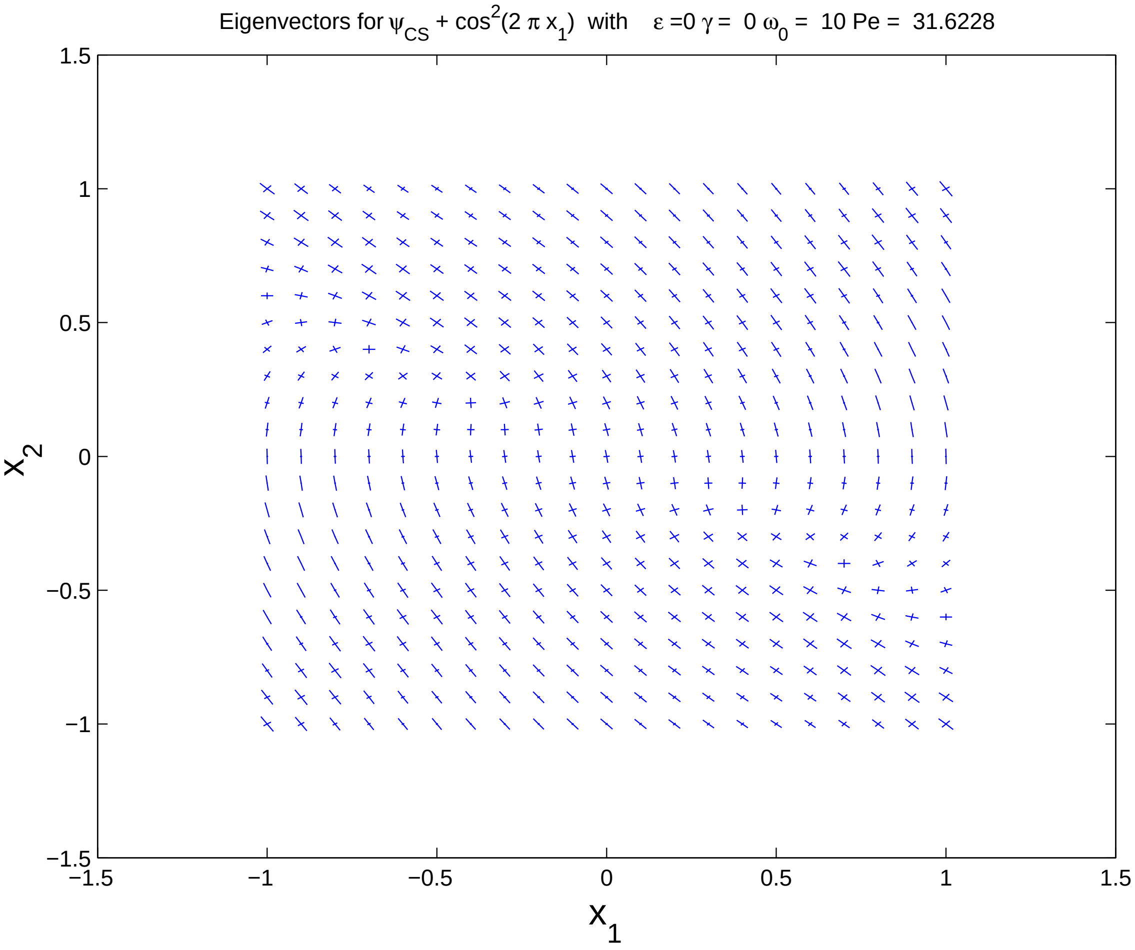

Figure 14: Effective diffusivity $\mathcal{K}^*$ in mean vortex flow and modified cellular periodic fluctuations.

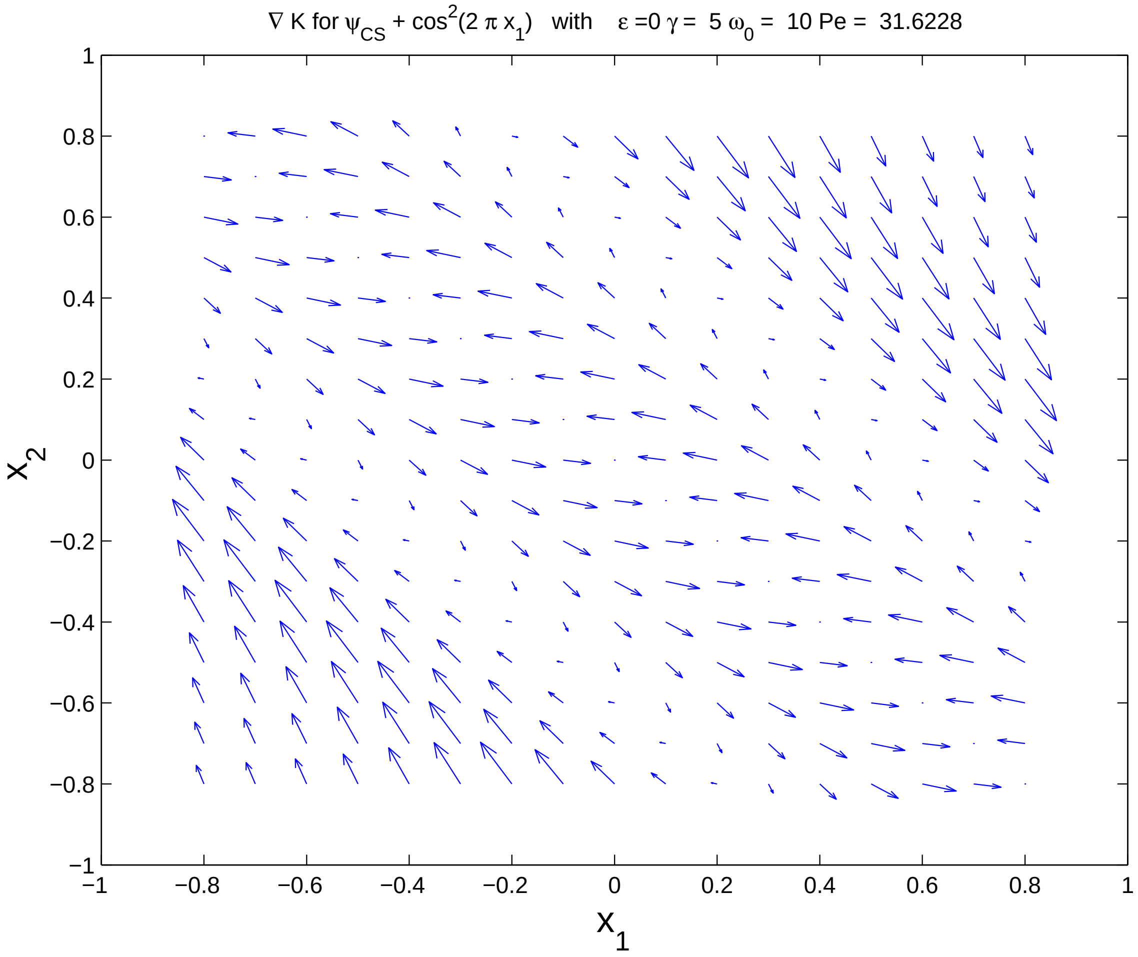

Figure 15: Drift correction $\nabla\cdot\mathcal{K}^*$ in mean shear flow and modified cellular periodic fluctuations.

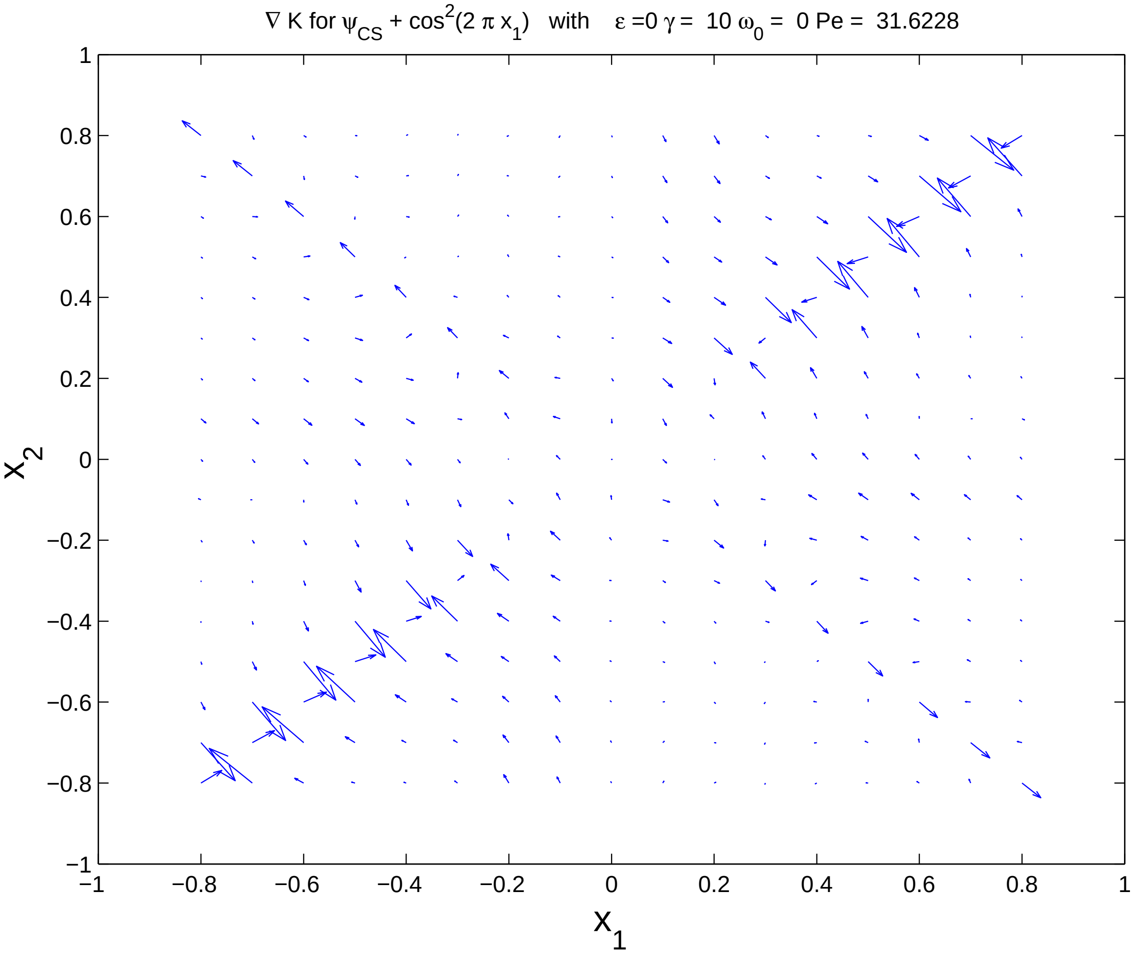

Figure 16: Drift correction $\nabla \cdot \mathcal{K}^*$ in mean strain flow and modified cellular periodic fluctuations.

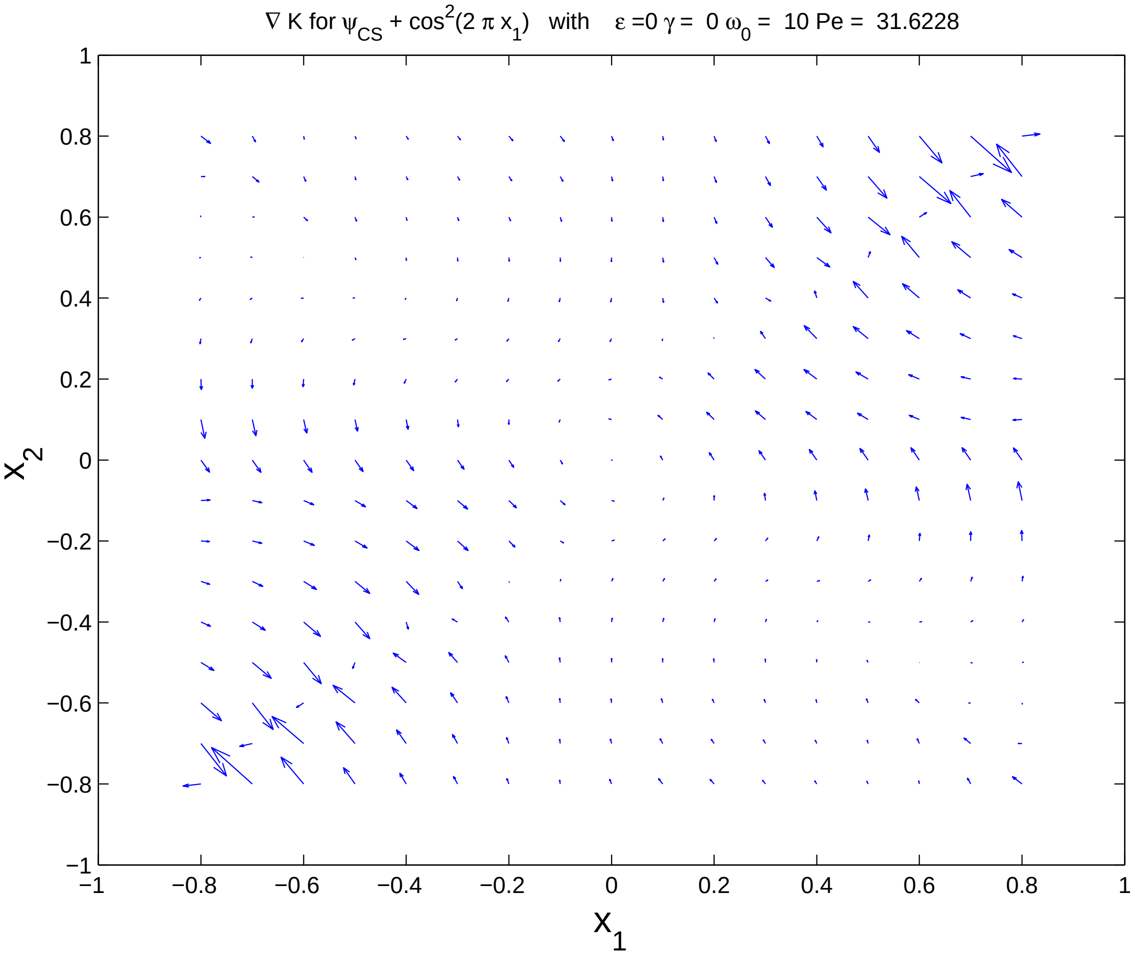

Figure 17: Drift correction $\nabla\cdot\mathcal{K}^*$ in mean vortex flow and modified cellular periodic fluctuations.

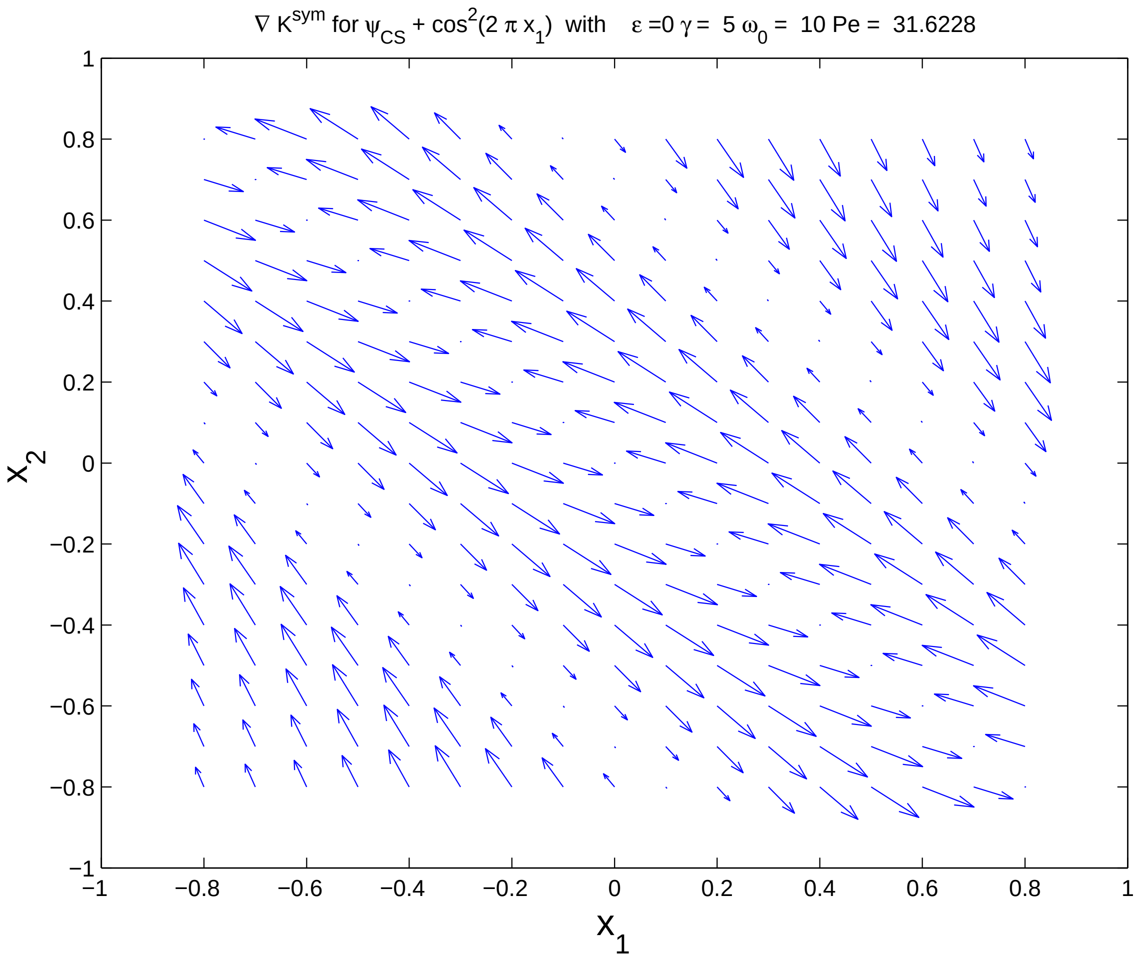

Figure 18: Symmetric contribution to drift correction $\nabla \cdot \mathcal{K}^{*(s)}$ in mean shear flow and modified cellular periodic fluctuations.

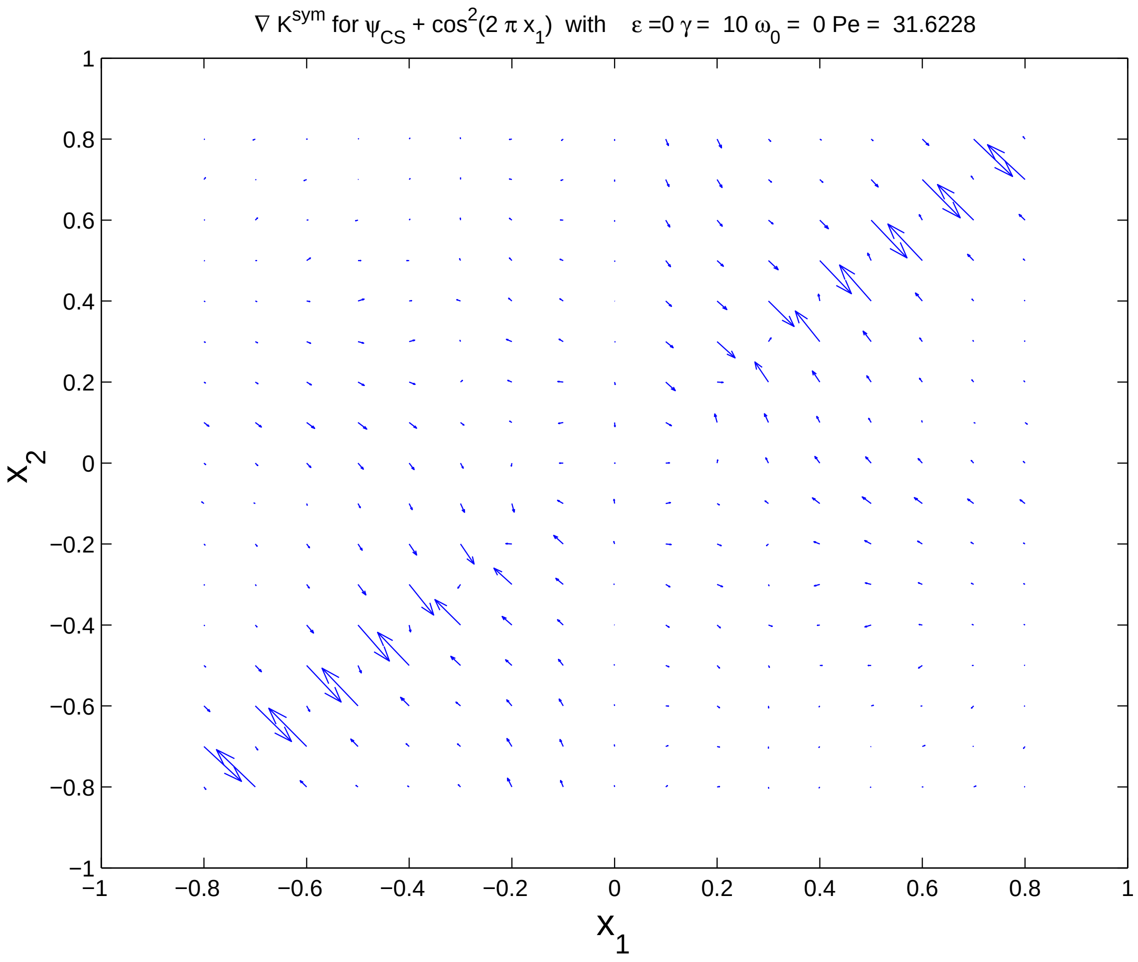

Figure 19: Symmetric contribution to drift correction $\nabla \cdot \mathcal{K}^{*(s)}$ in mean strain flow and modified cellular periodic fluctuations.

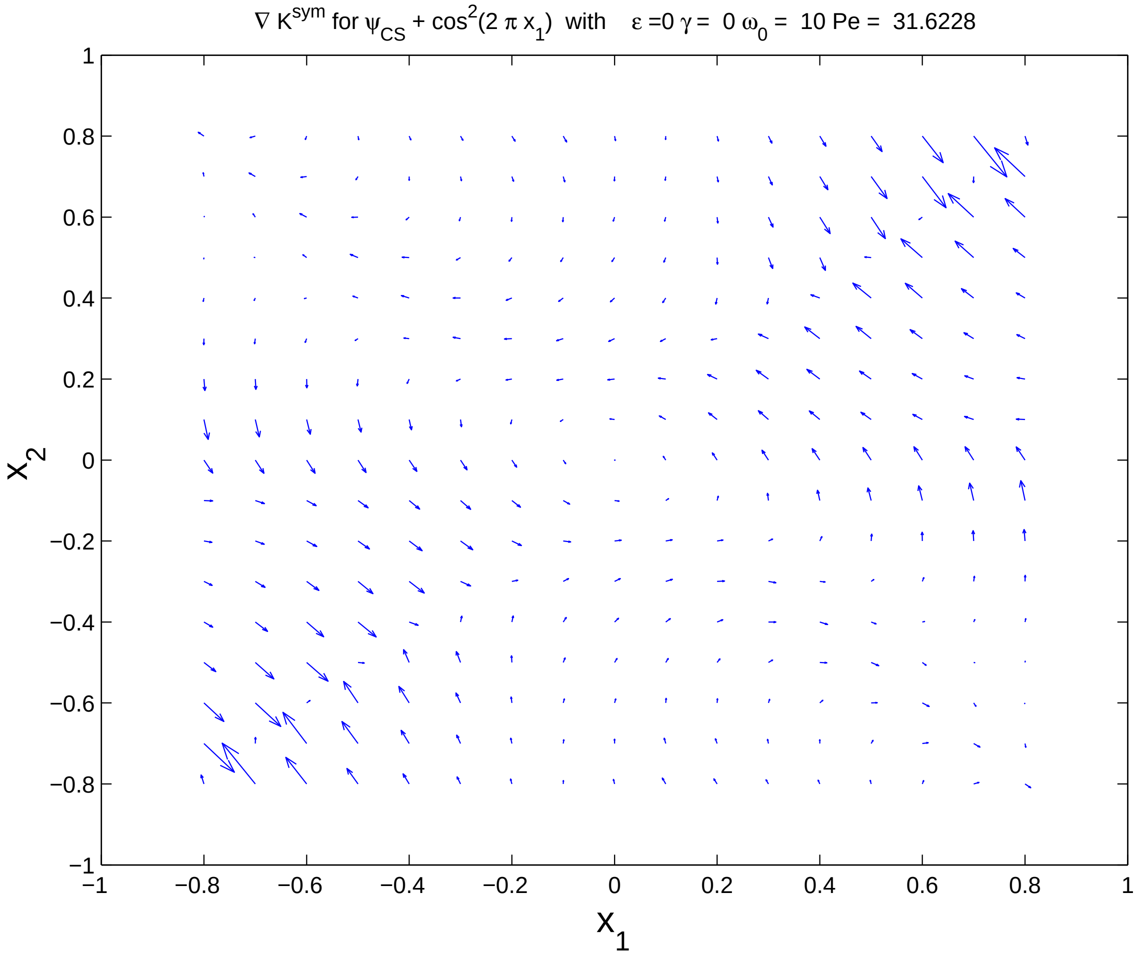

Figure 20: Symmetric contribution to drift correction $\nabla \cdot \mathcal{K}^*$ in mean vortex flow and modified cellular periodic fluctuations.

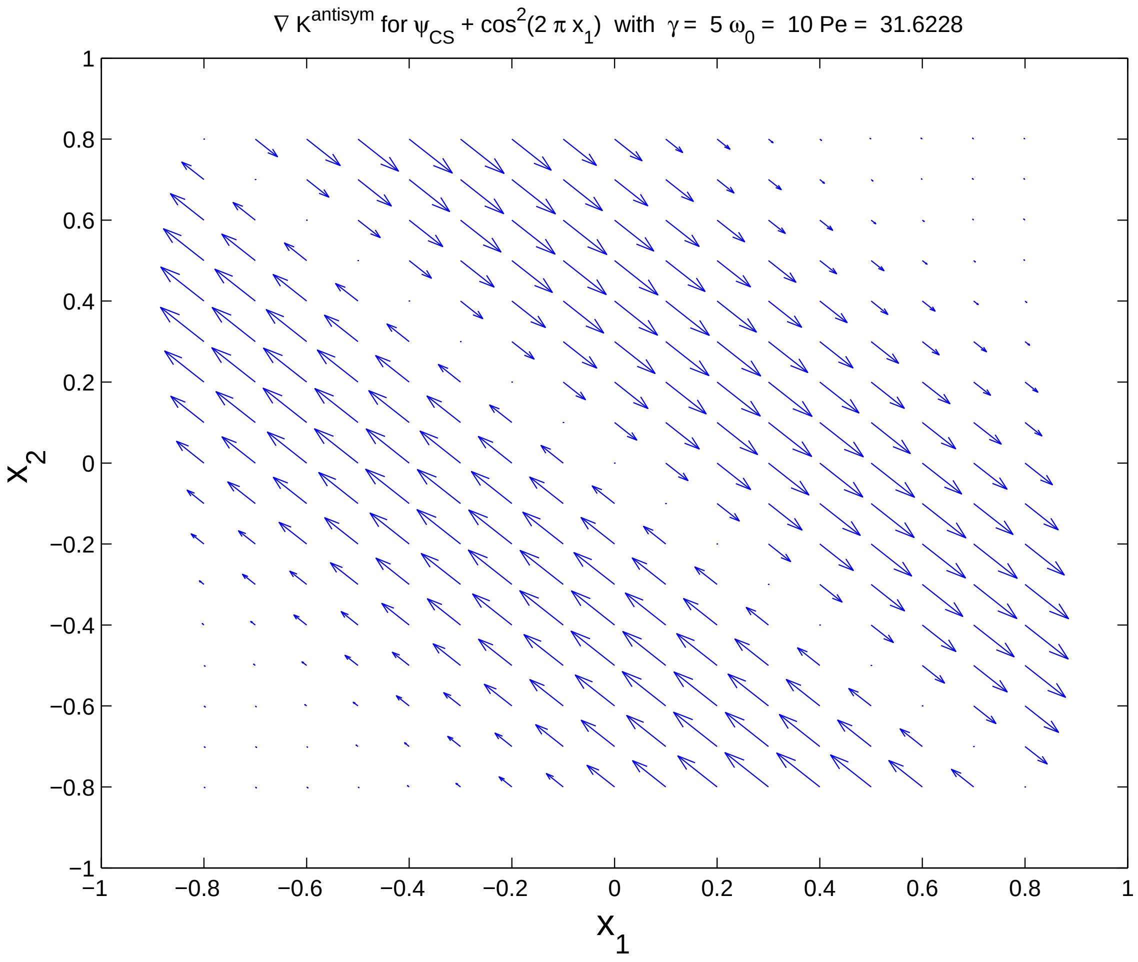

Figure 21: Anti-symmetric contribution to drift correction $\nabla\cdot\mathcal{K}^{*(a)}$ in mean shear flow and modified cellular periodic fluctuations.

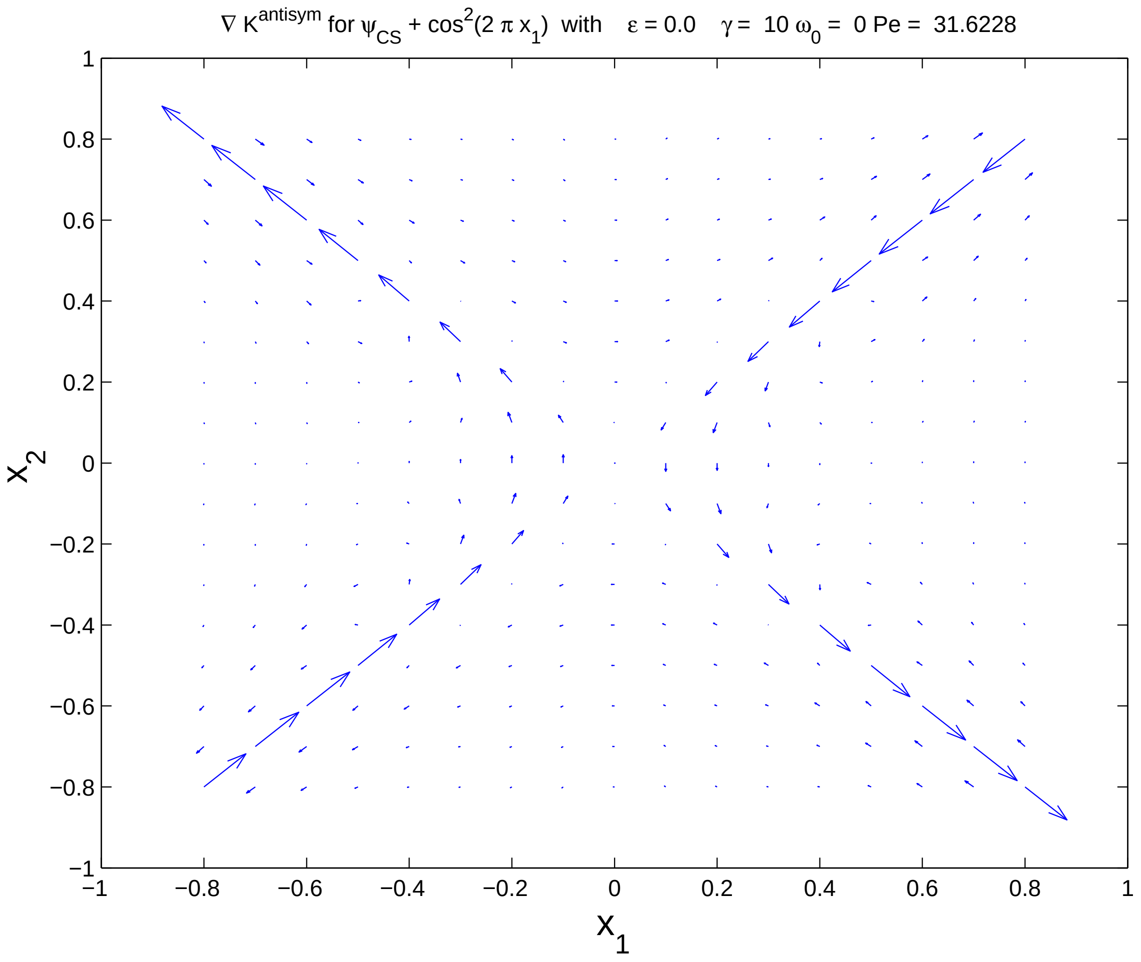

Figure 22: Anti-symmetric contribution to drift correction $\nabla \cdot \mathcal{K}^{*(a)}$ in mean strain flow and modified cellular periodic fluctuations.

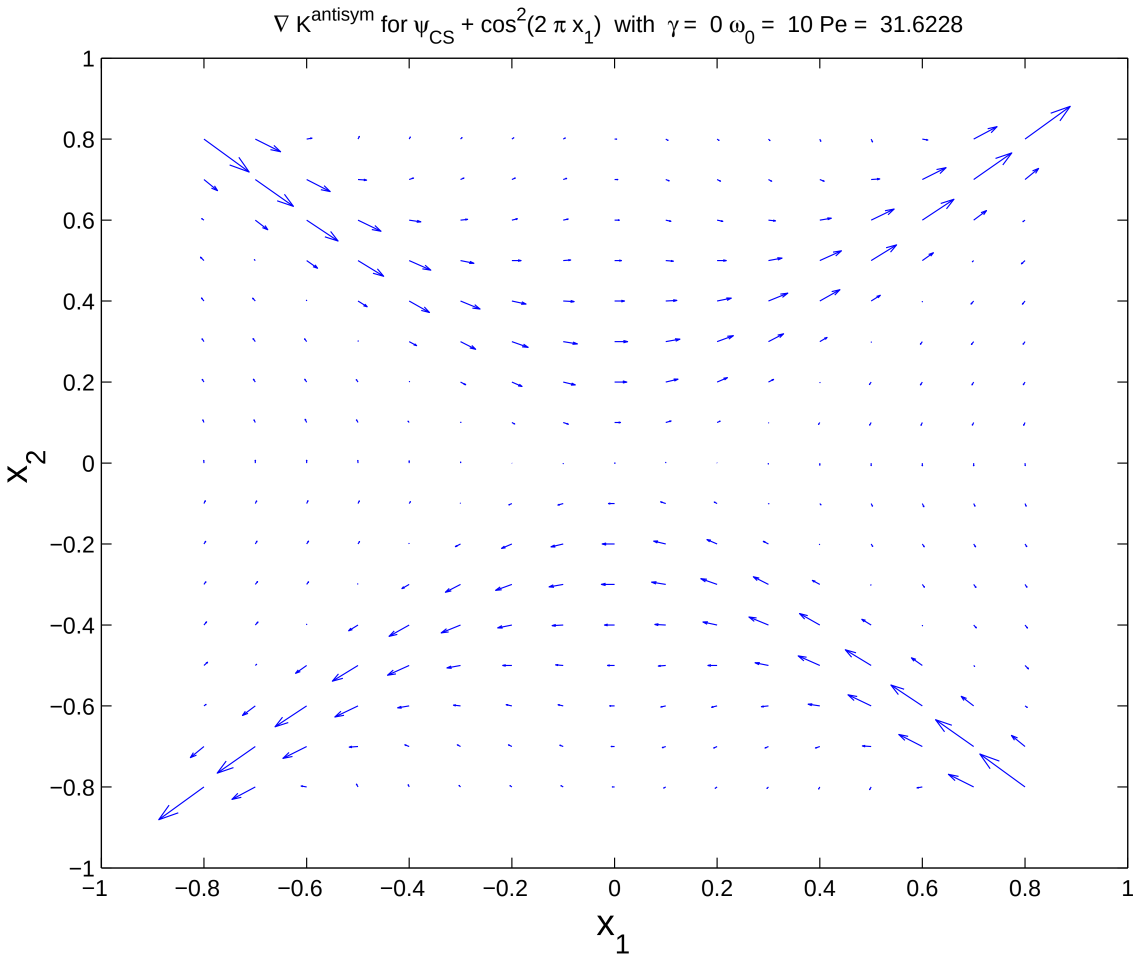

Figure 23: Anti-symmetric contribution to drift correction $\nabla \cdot \mathcal{K}^{*(a)}$ in mean vortex flow and modified cellular periodic fluctuations.

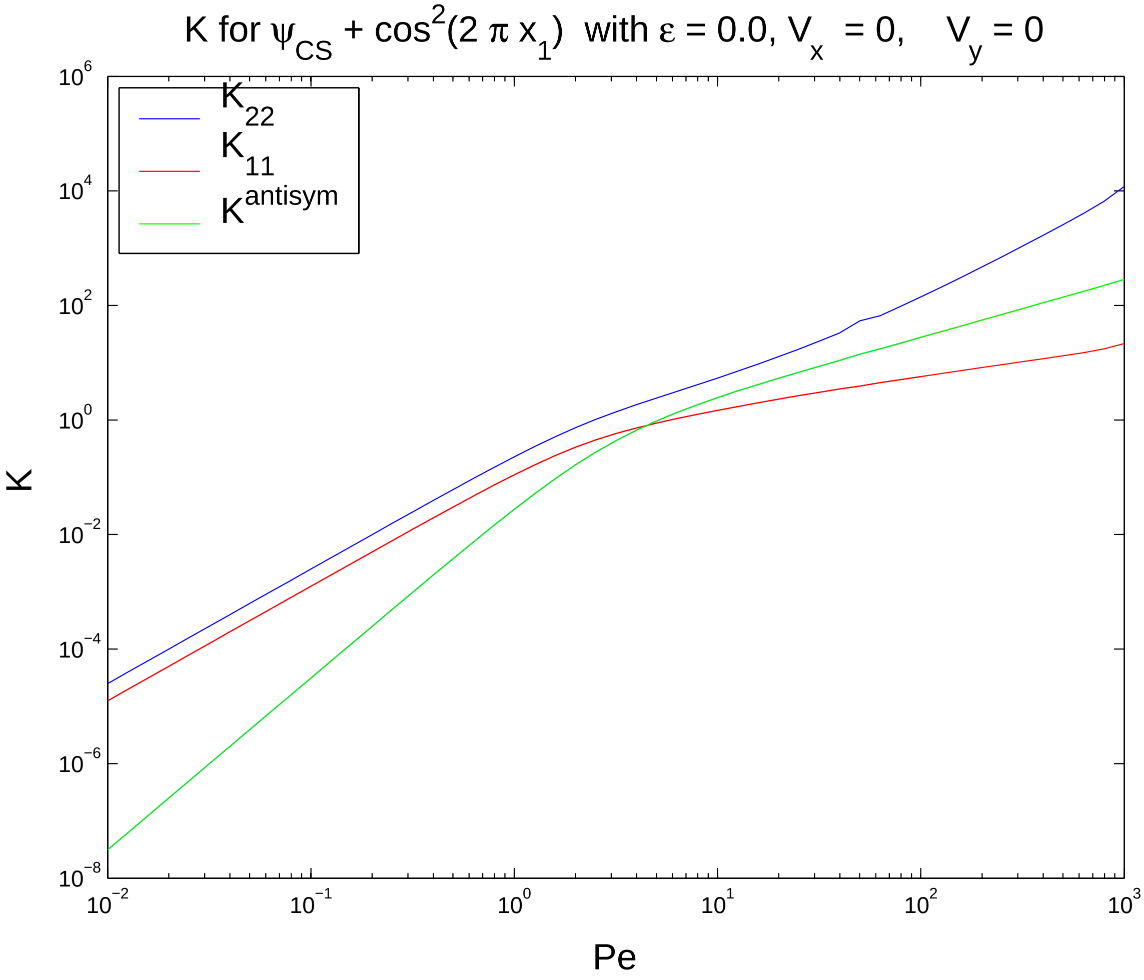

Figure 24: Symmetric and anti-symmetric components of effective diffusivity $\mathcal{K}^*$ for modified cellular flow with no mean flow.

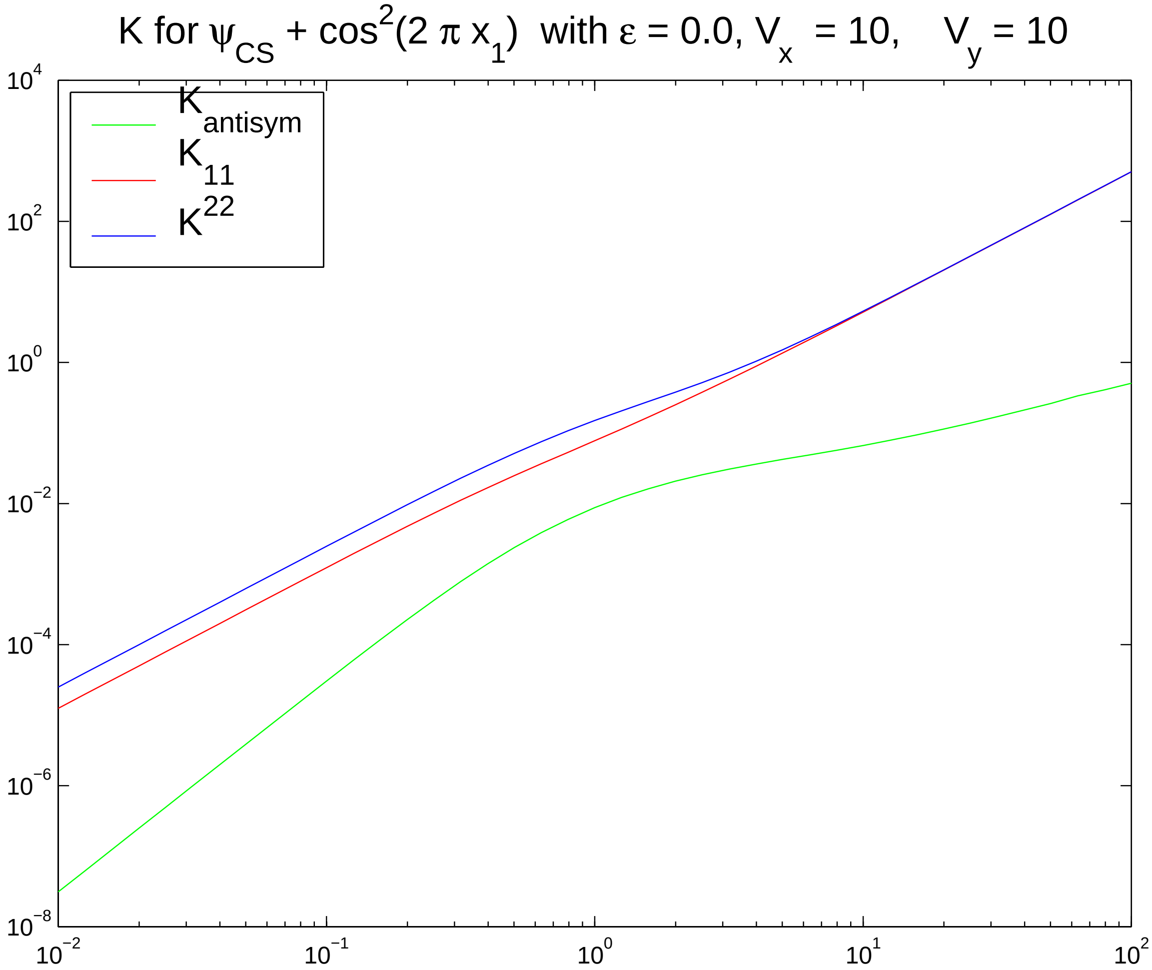

Figure 25: Symmetric and anti-symmetric components of effective diffusivity $\mathcal{K}^*$ for modified cellular flow with rational mean flow ratio.

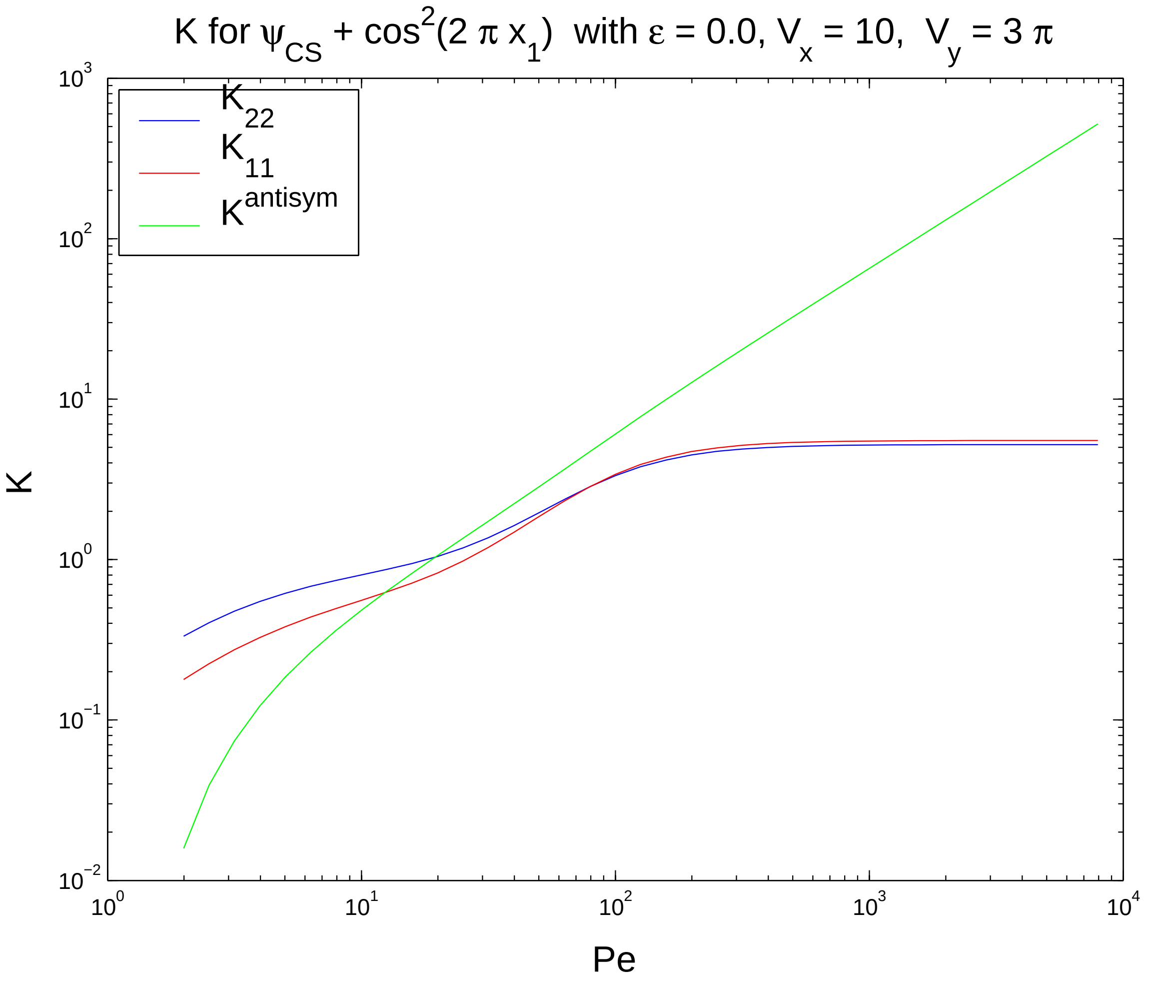

Figure 26: Symmetric and anti-symmetric components of effective diffusivity $\mathcal{K}^*$ for modified cellular flow with irrational mean flow ratio.

References

[1] Marco Avellaneda and Andrew J. Majda. Approximate and exact renormalization theories for a model for turbulent transport. *Phys. Fluids A*, 4(1):41–56, January 1992.

[2] James Bonn and Richard M. McLaughlin. Sensitive enhanced diffusivities for flows with fluctuating mean winds: a two-parameter study. *J. Fluid Mech.*, 445:345–375, 2001.

[3] P. Castiglione, A. Crisanti, A. Mazzino, M. Vergassola, and A. Vulpiani. Resonant enhanced diffusion in time-dependent flow. *J. Phys. A*, 31:7197–7210, 1998.

[4] Peter R. Kramer, Andrew J. Majda, and Eric Vanden Eijnden. Closure approximations for passive scalar turbulence: A comparative study on an exactly solvable model with complex features. Submitted to *J. Stat. Phys.*, December 7 2001.

[5] Marcel Lesieur. *Turbulence in fluids*, chapter 5.4, 5.5, pages 161–163. Number 1 in Fluid Mechanics and its Applications. Kluwer, Dordrecht, second revised edition, 1990.

[6] Andrew J. Majda and Peter R. Kramer. Simplified models for turbulent diffusion: Theory, numerical modelling and physical phenomena. *Phys. Rep.*, 314(4–5):237–574, June 1999.

[7] Andrew J. Majda and Richard M. McLaughlin. The effect of mean flows on enhanced diffusivity in transport by incompressible periodic velocity fields. *Stud. Appl. Math.*, 89(3):245–279, 1993.

[8] A. Mazzino. Effective correlation times in turbulent scalar transport. *Phys. Rev. E*, 56(5):5500–5510, November 1997.

[9] W. D. McComb. *The physics of fluid turbulence*, volume 25 of *Oxford Engineering Science Series*. Clarendon Press, New York, 1991.